

STOPOVER HOTSPOTS FOR MIGRATORY BIRDS IN NORTH AND CENTRAL AMERICA

SHI FENG¹, QINMIN YANG^{1*}, HUIJIE QIAO^{2*}, LUIS E. ESCOBAR³, XUAN YAN⁴

¹*State Key Laboratory of Industrial Control Technology, College of Control Science and Engineering, Zhejiang University, Hangzhou, 310007, PR China.*

²*State Key Laboratory of Animal Biodiversity Conservation and Integrated Pest Management, Institute of Zoology, Chinese Academy of Sciences, Beijing, 100101, PR China.*

³*Department of Fish and Wildlife Conservation, 1015 Life Science Cir, Virginia Tech, Blacksburg, VA 24061, USA.*

⁴*Independent researcher, 7912 Heritage Palms TRL, McKinney, TX 75070, USA.*

Abstract. Despite the large body of literature on avian migratory behavior, there is little information about stopover sites during bird movement, including the population-level drivers of breeding grounds and wintering grounds. Stopovers play an essential role in bird migratory site chains for energy supply and rest. There is an urgent need to identify and protect stopover sites to secure the long-term sustainability of migratory network connectivity and stability. To address this challenge, we reconstructed a migration network and identified geographic hotspots denoted as stopover sites. And we analyzed the high-density population movements of 52 focal migratory bird species using comprehensive observation data from eBird through PageRank algorithm. Furthermore, potential alternative stopover sites were explored using a word embedding technique based on geo-functional similarity. Our study was conducted in North and Central America during a three-year period and revealed three key stopover areas, including Florida peninsula and its inland, the region of Central America, and the region near Puget Sound. Results from this study can be used for conservation prioritization guidance, active surveillance of bird pathogens, and bird management.

Keywords: Central America, bird conservation, eBird, migration network, stopover

INTRODUCTION

Understanding migration pathways is critical for bird management and conservation. Migratory birds travel thousands of miles between breeding and wintering grounds, facing numerous threats along their routes, including habitat loss, climate change, and hunting (Nemes et al., 2023). By analyzing migration pathways, conservationists can identify key stopover sites and habitats that are essential for bird survival. Information about key stopover sites enables the creation of targeted protection strategies, such as establishing protected areas, restoring habitats, and implementing international agreements to safeguard migratory routes (Higuchi et al., 2012). Additionally, migration pathway studies can help predict the impacts of environmental changes on bird populations for proactive measures to mitigate potential threats (La Sorte et al., 2016) and to implement precision epidemiology of avian influenza.

Usually, migration depends on a suit of interconnected sites (Runge et al., 2015), and their conservation requires a deep understanding of the connectivity in migration networks. That is, untangling migration patterns requires to answer how migratory species connect their breeding and non-breeding grounds through their trajectories. Migratory connectivity can describe the spatiotemporal link of individuals and populations between sites caused by migratory movements, which can influence both long-term evolutionary responses and short-term population dynamics (Webster et al., 2002). Research on bird migratory connectivity generally focuses on geographical patterns that describe linkages between breeding and wintering grounds and the influencing drivers, such as resource requirements and ecological relationships (Kramer et al., 2018). Stopover sites, such as wetlands, forest fragments or grasslands, are essential for birds to rest and

*Corresponding authors: Qinmin Yang, Email: qmyang@zju.edu.cn, Huijie Qiao, Email: qiaohj@ioz.ac.cn

refuel during their migration journey. These sites are considered to be key nodes in migration network connectivity and require targeted attention (Guo et al., 2024). Traditionally, migration connectivity research relies on tracking techniques. For example, Knight et al. (2018) constructed a migration network for Tree Swallow (*Tachycineta bicolor*) with 133 geolocators to assess the spatial connection between wintering and breeding areas to help develop optimal conservation strategies in North America. Similarly, Xu et al. (2020) applied high-resolution GPS tracking data of 10 whooper swans (*Cygnus cygnus*), 81 swan geese (*Anser cygnoides*), 93 bar-headed geese (*Anser indicus*), and 54 greater white-fronted geese (*Anser albifrons*) with GPS loggers during 2005-2018 to study the migration network connectivity in the Central and East Asian-Australasian Flyways. Lastly, Catry et al. (2024) followed the migratory trajectories of 20 grey plovers (*Pluvialis squatarola*) with tracking devices to highlight important stopover sites and potential bottlenecks. These studies focused on the individual-level flyway and network, limiting the insight into population-level movements and being restricted to tracking costs and bird body size. Tracking a few individuals is not suitable for reconstructing the movement of a species. Similarly, individual tracking covers limited species due to the difficulty of capturing and carrying the track devices for small-sized ones.

Based on this data limitation of animal movement, broad-scale monitoring, such as radar or citizen science data, can provide comprehensive data for wider views of signals about the biogeography of bird movement. For example, Bonter et al. (2009) identified critical stopover sites with weather-surveillance radar images from 2000 to 2001 in the Great Lakes basin. Guo et al. (2024) applied five years of weather surveillance radar data to map the stopover densities of land birds during spring and autumn migration across the eastern United States. Radar data, however, fail to identify specific bird species and only provide information on total bird biomass. This coarse-scale estimation limits conservation and management strategies for specific bird species, and is subjected to the radar coverage region. Ai et al. (2024) developed a portable stereo vision observer for bird flocks in field scenarios based on feature and sensor methods. In their study, Ai et al. captured birds natural flocking behaviors such as foraging and convergent flying in mudflats and seashores, which is helpful for stopovers detection. Nevertheless, observer activities are assumed to be scenario-oriented and can be disturbed by temperature and wind, and this observer focuses on short-term movement of specific individuals within the observation site, failing to capture dynamics of the long-distance migration process.

eBird (<https://ebird.org/>) is the world's largest bird-watching data repository and has comprehensive information on the distribution and movement patterns of avian species at the population level. Lin et al. (2020) used eBird data to discover Priority Stopover Sites (PSSs) and quantified the potential benefit for resident species in terms of species abundance focusing on three North American countries, including Canada, the United States (US), and Mexico. Nicol et al. (2023) proposed a hidden semi-Markov model to infer crucial stopover nodes based on count data from eBird to estimate the most likely migration links among regions for an endangered shorebird named Far Eastern curlew (*Numenius Madagascariensis*) in the East Asian-Australasian Flyway. The current literature on stopover sites, however, evaluates the importance of sites based on population abundance or potential distributions combining the site protection status in isolation, but not from a systematic perspective. The spatial and temporal information of linkages among stopover sites for multiple species within a migratory network is usually overlooked. For example, Zhang et al. (2023) explored the backbone nodes of migration network among different regions using data from the Global Biodiversity Information Facility (GBIF, <https://www.GBIF.org/>) for 1862 species in 26 bird orders. In their study, Zhang et al identified the relative importance of nodes by betweenness (Wang et al., 2008) which is the number of shortest paths passing through the individual nodes in a network. The Zhang et al study, however, focused on the role that nodes play in the shortest paths of the network rather than paths across the network. Therefore, methods to comprehensively reconstruct overall stopover site connection are needed for biologically realistic migration network analysis (Wyborn and Evans, 2021). PageRank algorithm and word embedding technique can help address the need of more accurate network modeling methods for stopover detection.

PageRank was originally used for webpage ranking in Google (Page et al., 1999), where PageRank considers the number of connections to a webpage (represents a node in the users' clicking network). PageRank emphasizes the position and link relationship of nodes in the overall structure of the network. It measures node importance by analyzing the relationship between nodes, accounting for multiple indicators such as linkage quantity and quality, link distribution, damping factor, and initial PageRank, among others. Through the comprehensive calculation of these indicators, PageRank can determine the relative importance of nodes in the network. Usually, nodes linked to a high-PageRank node will have an increasing PageRank value and are considered more important in the network. In human society networks, PageRank values have been

used to identify important user social nodes (Hong et al., 2023), and analyze urban mobility network (Wang et al., 2017).

Word embedding is a natural language processing (NLP) technique used to represent words as dense vectors (Mikolov et al., 2013). These vectors capture semantic relationships and contextual information about words, allowing computers to process and understand human language more effectively. Word embedding methods have been widely used for vector representations of words in documents, social analyses, and location analyses in human society (Jin et al., 2014). Mikolov et al. (2013) introduced word2vec algorithm to represent each word as a vector using large-scale document datasets. Words with similar contexts will have similar representations in the vector space. It is popular in the NLP applications, including machine translation (Qian et al., 2019), citation visualization (Berger et al., 2016), and sentiment analysis (Liu et al., 2020; Xiong et al., 2018). Meanwhile, the method has also been widely applied in human mobility data for geo-functional similarity exploration based on semantic similarity (Zhu et al., 2019), where a location can be defined as a word, and a set of successive and previous locations in a trajectory can be defined as its context. Considering that trajectory data is a type of sequential data, exploring the function of a location through its context is similar to understanding the meaning of a word in a sentence. For example, Zhu et al. (2019) proposed a location representation Location2vec method based on word2vec to capture the similarity relationships among locations.

Based on these, the aim of this work was to investigate the stopover hotspots during the bird migration process and identify alternative stopover sites to increase the site connectivity along bird migratory networks. We assessed the importance of stopover sites with the network-level linkage quantity and quality through the PageRank algorithm. This study provides a comprehensive population-level understanding for migration trajectories for diverse taxa using eBird data. We introduced the word embedding technique to analyze trajectory sequence contexts and detected potential alternative sites based on geo-functional similarity. Discovery of specific stopover hotspots are expected to inform migratory bird conservation, surveillance, and management for North and Central America birds.

MATERIALS AND METHODS

Data acquisition and preparation

Bird occurrence data for 52 focal migratory bird species (Table S1) were collected from the eBird (<https://>

ebird.org/) citizen-science database for the period 2017-2022. The 52 migratory species are selected from 82 focal species list (Schrimpf et al., 2021) where observation data are abundant for analysis. Data from 2017-2019 worked as the study dataset, and the data from 2020-2022 were used for network validation. Observation data covered continental North and Central America with metadata including date and location (longitude and latitude) for each record. The study was carried out in MATLAB R2021b for PageRank value calculation, and Python 3.10 for trajectory estimation and word2vec analysis. The specific packages are shown below for the full process: *pandas* (version 1.4.3; Reback et al., 2022), *numpy* (version 1.23.5; Harris et al., 2020), *datetime* (version 4.4), *matplotlib* (version 3.5.3; Hunter, 2007), *xlwt* (version 1.3.0; Machin, 2017), *pyproj* (version 3.3.1; Whitaker, 2022), *pygam* (version 0.8.0; Marin, 2018), *scikit-learn* (version 1.1.2; Grisel et al., 2022), *basemap* (version 1.3.4; Whitaker, 2022), *tqdm* (version 4.65.0; Yorav-Raphael & da Costa-Luis, 2024), *xlrd* (version 2.0.1; Withers, 2020), *openpyxl* (version 3.1.2; Gazoni & Clark, 2023), *genism* (version 4.3.1; Rehurek, 2023), and *xlwings* (version 0.30.6; Zumstein, 2023).

We randomly subsampled the original dataset to retain 100 records per day to keep the balance between computation cost and information available. Migration trajectories of high-density populations for each species during each migration cycle were estimated using a minimum cost analysis (Feng et al., 2021; Somveille et al., 2021). Data were first preprocessed through mean location interpolation for observations of missing dates, using rolling-window smoothing (Zivot and Wang, 2007), and outliers were detected and removed using Space Local Deviation Factor algorithm (Zhang and Wang, 2011). Observations were then discretized by Mean-shift clustering algorithm (Dermanis, 2005) for dense population centroids. Centroids were grouped according to the minimum cost principle and trajectories were fitted using a Generalized Additive Model (Hastie and Tibshirani, 1990).

Migration trajectory sequence conversion

To convert the migration trajectories into geographic cell-ID sequences, we set an origin point in position (0.1° N, 134.2° W) which was (10799.54, -14796209.33) in the Spherical Mercator map (Fig.1), and built a grid coordinate system for 35×36 cells divided by: $(-14796209.33 + 200000m, 10799.54 + 200000n)$ where $m \in [1, 35]$, $n \in [1, 36]$ to cover the continental North and Central America (Fig.1). Then the number for each cell was calculated by: $m + 35 * (n - 1)$.

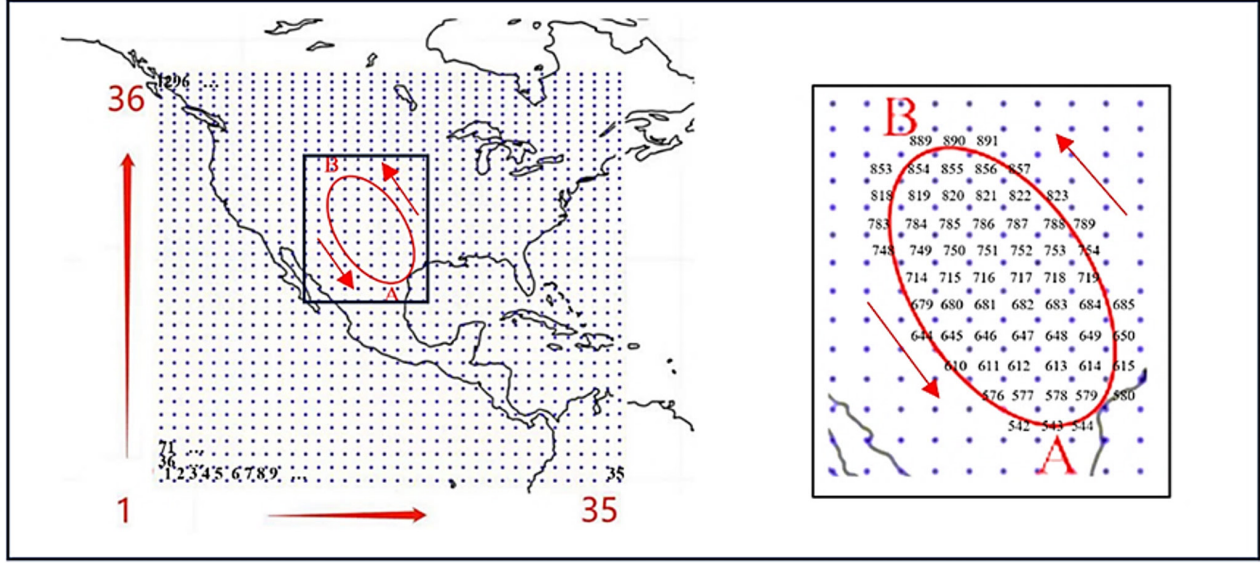


Figure 1. Schematic diagram for geographic partition by building 35×36 cells to cover continental North and Central America. The number for each cell is 1-35 in the bottom line, then 36-70 for the second line, and so on. Through the grid coordinate system after geographic partition, trajectories are presented as geographic cell-ID sequences according to daily locations. For example, the ellipse trajectory in the diagram above can be represented by a sequence from point A to point B and back to point A as follows (sojourn time ignored): 543-544-580-615-650-684-719-754-788-822-856-891-854-818-783-748-714-679-644-610-576-542-543.

Migration network construction and stopover hotspots mining

In this study, each geographic cell was defined as a node in the migration network with links resulting from cells with occurrences in adjacent positions in trajectory sequences. Node importance in the bird migration network was assessed through birds' movement between cells with the PageRank algorithm. We set the initial PageRank values for all nodes as $1/N$, where N was the total number of nodes (Rogers, 2002). In order to avoid infinite iteration, it is usually necessary to set a convergence threshold. That is, if the PageRank value of each web page changes less than a preset threshold (0.0001 in our case), its value is considered to have converged, and the iteration can be stopped. Alternatively, by setting the maximum number of iterations as an iteration termination condition (100 in our case). The damping factor is constant with an empirical value of 0.85, which is used to simulate the movement probability between different nodes and avoid the problem of infinite loops. After setting the movement relationship between nodes, the PageRank value calculation result of each node can be obtained according to the set threshold and the maximum number of iterations. PageRank values could represent the relative importance of each node in the migration network, which was used for node ranking. The mathematical expression for PageRank algorithm is:

$$PR(node_A) = (1-d) + d \left(\sum_i \frac{PR(node_{B_i})}{L(node_{B_i})} \right)$$

where, $PR(node_A)$ is the PageRank of node A; d is the damping factor; $PR(node_{B_i})$ are the PageRank values of nodes that link to node A; $L(node_{B_i})$ is the number of outbound links on node B_i .

The cells in the grid coordinate system after geographic partition in this study were considered as nodes and the sequence of trajectories formed links between different nodes to construct a migration network. We defined nodes with the sojourn time between 5-20 days in the trajectory sequences as stopover sites based on the empirical distribution of bird stopover days during migration (Kaiser, 1999; Fig.S1). This stopover period allowed us to differentiate stopover sites from breeding and wintering sites.

Potential alternative stopover sites exploration

Cell-ID sequences were analyzed using a word embedding technique to explore the potential alternative sites for stopover hotspots identified through PageRank algorithm. A cell-ID in the trajectory sequence was defined as a word, while a trajectory sequence was defined as a sentence, with multiple trajectories defined as a document corpus. This ensemble of cells allowed us to encode a migratory trajectory as:

$$tr = \{cell-ID_1, cell-ID_2, \dots, cell-ID_k, k = 1, 2, \dots\}$$

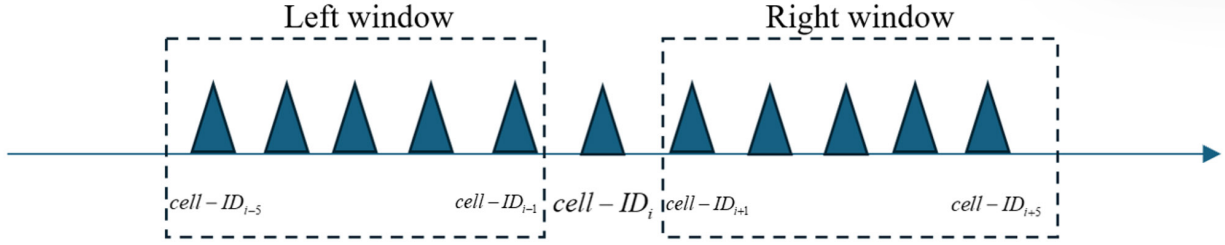


Figure 2. A diagram for the context of a word with the window size is five. The context of a word $cell-ID_i$ with its window size is five can be defined as: $context(cell-ID_i) = \{cell-ID_{i-5}, \dots, cell-ID_{i-1}, cell-ID_{i+1}, \dots, cell-ID_{i+5}\}$, where a contextual word ($cell-ID_c$) can be one of $cell-ID_{i-5}, cell-ID_{i-4}, cell-ID_{i-3}, cell-ID_{i-2}, cell-ID_{i-1}, cell-ID_{i+1}, cell-ID_{i+2}, cell-ID_{i+3}, cell-ID_{i+4}, cell-ID_{i+5}$.

All the trajectory sequences were encoded as:

$$TR = \{tr_1, tr_2, \dots, tr_n, n = 1, 2, \dots\}$$

Then we confined the context of word $cell-ID_i$ as:

$$context(cell-ID_i) = \{cell-ID_{i-m}, cell-ID_{i-(m-1)}, \dots, cell-ID_{i-1}, cell-ID_{i+1}, \dots, cell-ID_{i+(m-1)}, cell-ID_{i+m}\}$$

where m is the window size. Figure 2 shows a case when the window size is set as five.

We applied the Skip-Gram model (McCormick, 2016), which is part of word2vec (Mikolov et al., 2013), to build word representations (embeddings) that can predict the surrounding context words for a given target word. Skip-Gram model can help capture the semantic relationships between words, discovering the geo-functional similarity relationship between sites in the migration network. The model takes a target word as input and predicts the previous and following words expected to appear in the context. Word prediction is conducted using a user-specified window size. Model training involves adjusting the word embeddings to maximize the probability of correctly predicting the context words surrounding the target word. Here, we defined the object of the Skip-Gram model to maximize the average log probability as:

$$L = \sum_{cell-ID \in A} \log p(context(cell-ID) | cell-ID)$$

where A is all the words in the document corpus, $context(cell-ID)$ is the context of the word $cell-ID$ with its size $2m+1$. We then moved a contextual window of length $2m+1$ across the documents to maximize the co-occurrence probability of the words that appeared within a window. We assumed that the sequence of words was identically distributed and independent, where the probability of its contextual words was:

$$p(context(cell-ID) | cell-ID) = \prod_{cell-ID_c \in context(cell-ID)} p(cell-ID_c | cell-ID)$$

where $cell-ID_c$ is a contextual word of $cell-ID$.

The probability of $p(cell-ID_c | cell-ID)$ was calculated with SoftMax function:

$$p(cell-ID_c | cell-ID) = \frac{v_c^T v_{cell-ID}}{\sum_{u \in W} v_u^T v_{cell-ID}}$$

where $cell-ID_c, cell-ID_u, cell-ID$ are the vectors of word $cell-ID_c, cell-ID_u, cell-ID$, W denote the set of all words. $cell-ID_u$ is one of the total words, and "T" is the transposition for the vector of $cell-ID_u$, then the dot products of the vector $cell-ID$ and $cell-ID$ can be calculated.

In the Skip-Gram model, the computational complexity of the output layer was high because it required calculating the probability distribution over the entire vocabulary. Here, the vocabulary represented the entire datasets of cell-IDs, which was large and in turn, time-consuming. We applied a negative sampling to selectively update model parameters (Mikolov et al., 2013), allowing the model to update only a small subset of parameters in each training step. The negative samples accelerated the training process. For the target word represented by $cell-ID$ in the formula, we selected its contextual words $context(P)$ as positive samples and P words that did not belong to $context(cell-ID)$ as negative samples (Zhu et al., 2019). A logistic regression was applied to train the model using positive and negative samples, aiming to maximize the prediction probability for positive samples while minimizing it for negative samples. We defined the object function as:

$$L = \sum_{cell-ID \in A} \sum_{x \in context(cell-ID)} \left[\log \sigma(v_x^T v_{cell-ID}) + \sum_{cell-ID_p \in NEG(cell-ID)} \log(1 - \sigma(v_p^T v_{cell-ID})) \right]$$

where:

$$\sigma(x) = \frac{1}{(1 + \exp(-x))}$$

$v_x, v_p, v_{cell-ID}$ is the vectors of word $cell-ID_x, cell-ID_p, cell-ID$. We use $cell-ID_x$ to present a word included in the context of $cell-ID$ and use $cell-ID_p$ to present a word not included in the context of $cell-ID$. “T” also presents the transposition of the vector for dot products between vectors.

Finally, a high-dimensional vector for each word was got after optimizing the object function on the trajectory documents. The similarity of two vectors v_a, v_b was then calculated with the cosine distance in the vector space as:

$$\text{Similarity}(v_a, v_b) = \frac{\vec{v}_a \cdot \vec{v}_b}{\|\vec{v}_a\|_2 \cdot \|\vec{v}_b\|_2}$$

The cosine distance calculation results for similarity representation between each two high-dimensional vectors in the trajectory corpus were shown in the heat map for geographic interpretation. Geo-functional similarity mining was done by finding the two cell-IDs closest to the important stopover sites (hotspots got through PageRank algorithm) in the vector space with the minimum cosine distances as the potential alternative stopover sites.

When applying word2vec for vector presentation, the following two parameter settings need to be noted:

- (1) Vector dimensionality: Low dimensionality usually means information loss. We set 100 as the embedding dimension to facilitate information preserving and compactness according to empirical knowledge and experiments.
- (2) Window Size: A larger window tends to capture more overall information, and a smaller window gets local syntactic contexts (Levy and Goldberg, 2014). For mobility data, a larger window reveals mobility behaviors, and a smaller window captures geographical similarity (Zhu et al., 2019). According to the length of trajectories, we set the window size as 5 to focus on the local geographical similarity of neighbor cells.

Analytical framework

The overall analytical framework is described in Figure 3. Migratory trajectories were estimated from field occurrence data in the form of geographic coordinates from the eBird repository (<https://ebird.org/>; Feng et al., 2021). Geographic coordinates of migration trajectories were analyzed as spatio-temporal words using a situation-aware

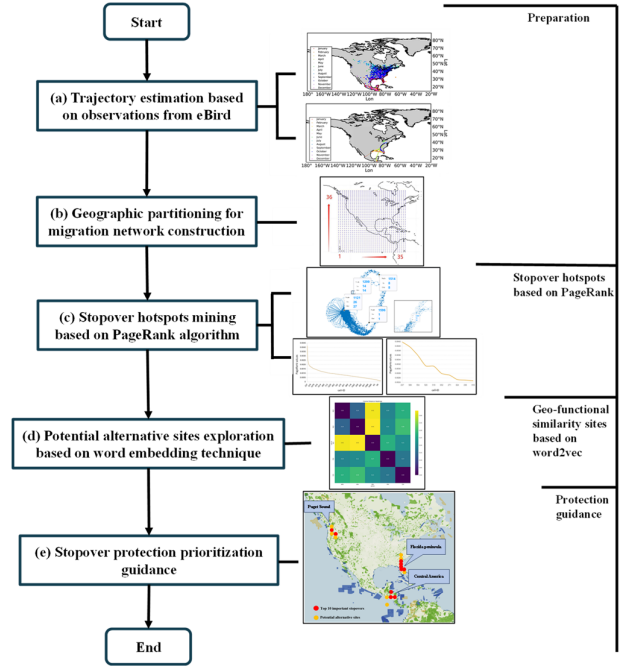


Figure 3. Overall structure for the method. (a) Trajectory estimation based on observations from eBird. The modelling process begins with estimating bird migration trajectories based on citizen-science observation data stored in eBird platform. The data collection forms the foundation for understanding the migration paths of birds. (b) Geographic partitioning for migration network construction. After estimating the trajectories, the migration routes are geographically partitioned, and a migration network can be constructed between different cells which form nodes, and edges represent the migration paths between these cells. (c) Stopover hotspots mining based on PageRank algorithm. The PageRank algorithm is then applied to the migration network to identify important stopover hotspots. PageRank ranks nodes based on their linkage quantity and quality, thereby identifying critical nodes, especially key stopover sites in the migration network. (d) Potential alternative sites exploration based on word embedding technique. A word embedding technique (word2vec) is used to explore potential alternative sites that have similar geo-functional properties to the identified stopover hotspots. This technique identifies locations that could serve as alternative stopover sites based on spatial and functional similarities. (e) Stopover protection prioritization guidance. Stopover protection prioritization can be inferred based on the stopover hotspots and alternative stopover sites. Right: (a)-(b) Preparation. The first two steps are part of the data preparation phase, which focuses on trajectory estimation and preparation for network construction. (c) Stopover hotspots based on PageRank. The third step utilizes the PageRank algorithm to rank and identify stopover hotspots. (d) Geo-functional similarity sites based on word2vec. The fourth step explores alternative sites with similar geo-functional characteristics using the word2vec technique. (e) Protection guidance. The final step is for stopover protection prioritization guidance based on sites predicted.

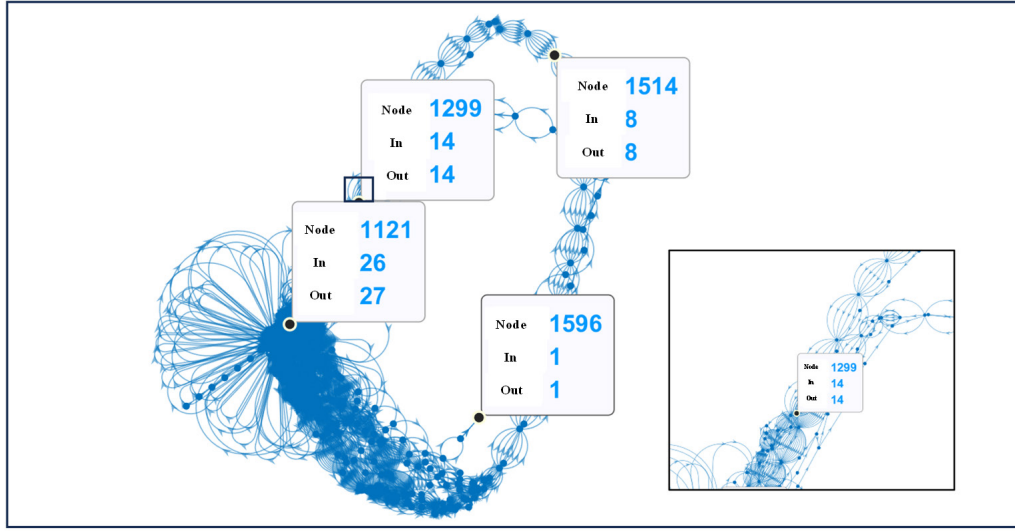


Figure 4. Migration network structure for 2017-2019. Each node can be located and show the in-degree and out-degree. Take node 1299 in the black square for example, it represents cell with number 1299 in the geographic partition map (Fig.1) with its in-degree and out-degree are 14. Arrows show movement direction between nodes. Inset: The in (out) degree can reflect the number of arrows move to (from) each node. The figure above can help us obtain the degree and structure information for each node in the migration network which works as the basis of PageRank algorithm.

analysis (Zhu et al., 2019). The situation-aware analysis assessed dynamic bird mobility across a grid coordinate system of continental North and Central America after geographic partition. Trajectory coordinates were converted to cell-ID (the number for each cell) sequences. Cell-ID sequences were used to build a migratory network with each cell as a node. Stopover hotspots were identified using the PageRank algorithm (Page et al., 1999) and potential stopover alternative hotspots were determined using a word embedding technique (Mikolov et al., 2013). Stopover hotspots and alternative stopover sites were projected on maps to identify areas for protection prioritization and analysis for migratory birds.

Stopover hotspots characteristics

The effect of landscape configuration on the network was explored based on landscape variables and stopover hotspots. We overlaid the artificial light (<https://www.nasa.gov/image-article/earth-night/>), the topographic map (<https://apps.nationalmap.gov/viewer/>), and the World Database on Protected Areas (<https://www.protectedplanet.net/en/thematic-areas/wdpa?tab=WDPA>) in North and Central America for protection prioritization reference. And we used the coverage of the total species and trajectory numbers to evaluate the stopover hotspots importance, and the overlapped species to assess the results of geographic functional similarity. Then we used the datasets of the Global Land Cover Estimation (GLanCE; Stanimirova

et al., 2023) product and Human Footprint (HFP) datasets (Mu et al., 2022) to analyze the land cover classes and the interference degree of human activities on the ecosystem about the stopover hotspot conditions quantitatively. Finally, we combined the stopover hotspot areas with the Important Bird and Biodiversity Areas (IBAs) in North and Central America (Donald et al., 2019; <https://datazone.birdlife.org/>) for protection strategy comparison.

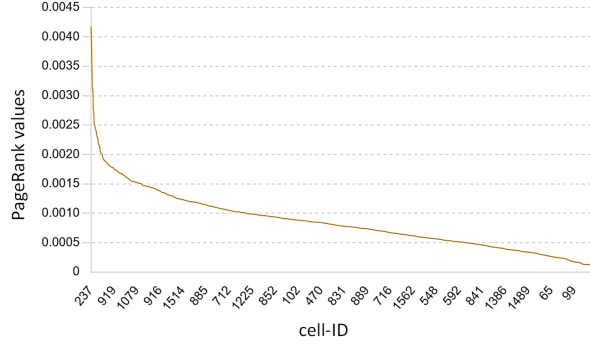
RESULTS

Migration network structure and PageRank value results

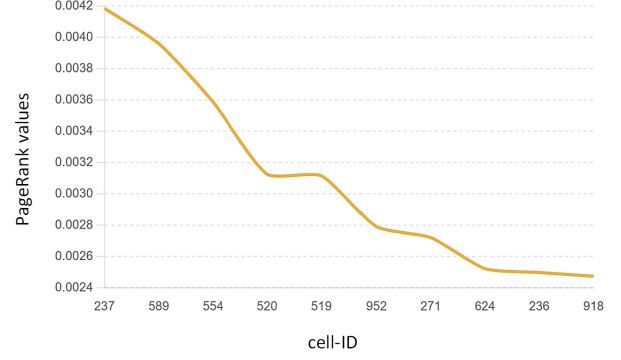
We modeled 52 migratory species during the period from 2017 to 2019, and estimated 540 migration trajectories in 2017, 435 in 2018, and 435 in 2019. The migration network structure resulted in a total of 1410 sequences during the study period (Fig.4), including their respective PageRank values at the cell level (Fig.5). The top 10 important stopovers nodes with the highest PageRank values were: cells 237, 589, 554, 520, 519, 952, 271, 624, 236, and 918.

Potential alternative stopover sites

A heatmap of cosine distance revealed calculation results between each two high-dimensional vectors of cells by word embedding technique (Fig.6). We performed geo-functional similarity mining for the top 10 important stopover cell-IDs (i.e., 237, 589, 554, 520, 519, 952, 271, 624, 236, 918) and the results were shown in Table 1.



(a) Curve for PageRank values of each cell



(b) Curve for the top 10 PageRank values of stopover cells

Figure 5. The PageRank value results. (a) The PageRank value curve of 1091 cell-IDs included in the avian trajectory sequences, which is ordered from the largest to smallest. The y-axis is the PageRank values, and the x-axis is cell-IDs; (b) The PageRank value curve for the top 10 important stopovers cells, where 10 cells: 237, 589, 554, 520, 519, 952, 271, 624, 236, 918 are included. Similarly, the y-axis is the PageRank values, and the x-axis is the cell-IDs of top 10 important stopovers.

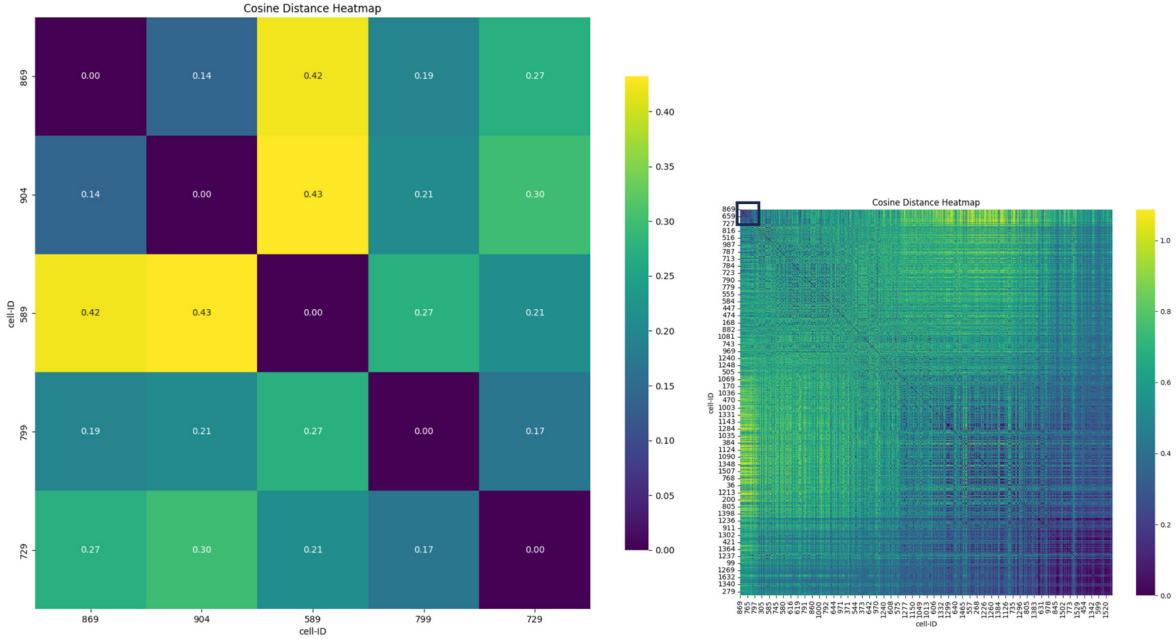


Figure 6. Heatmap of cosine distance between vectors of cells based on word2vec. The image on the left is a partial eagle eye diagram of the right one for a clearer presentation. The color of the grid can show the similarity between two cells. The smaller the cosine distance is, the higher the similarity is.

Table 1. Top 10 important stopovers and their potential alternative sites with cosine distances analysis for 2017-2019

Top 10 important stopovers	Potential alternative stopover sites (cosine distance based)	
237	236(0.0367)	165(0.0406)
589	659(0.1367)	624(0.1454)
554	519(0.1330)	624(0.1437)
520	519(0.0661)	485(0.0749)
519	520(0.0661)	485(0.1238)
952	917(0.0498)	987(0.0606)
271	237(0.0610)	236(0.0618)
624	659(0.1240)	694(0.1291)
236	235(0.0261)	237(0.0367)
918	883(0.0493)	952(0.0611)

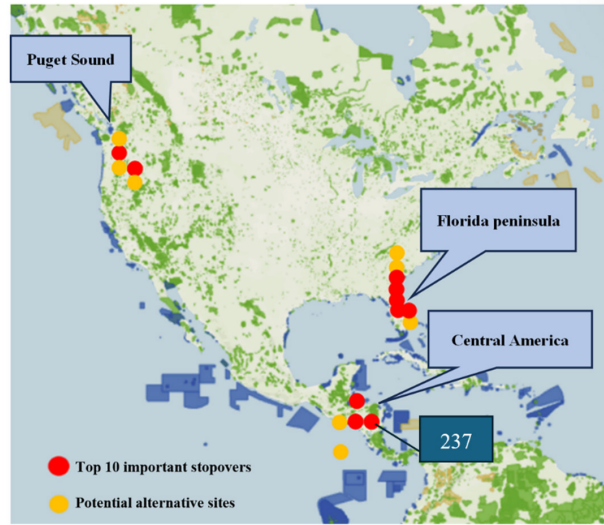


Figure 7. Stopover hotspots and potential alternative sites for them overlaid on the protected area map. The red solid circles represent the top 10 important stopovers acquiring the top 10 PageRank values. The orange circles represent potential alternative stopover sites. Green polygons denote terrestrial and inland water protected areas. Blue polygons represent marine protected areas. Three areas are highlighted and recommended as higher protection prioritization sites for targeted attention, including Florida peninsula and its inland, the region of Central America, and the region near Puget Sound.

Post modeling interpretation

The map for the stopover hotspots and their potential alternative sites in North and Central America (Fig.7) revealed three areas highlighted for higher protection prioritization: Florida peninsula and its inland (FL), the region of Central America (CA), and the region near Puget Sound (PS) rich in national parks and forests. The overlapped map with the artificial light map and topographic map can be found in Fig.S2.

In the stopover hotspots result assessment for 2017-2019, the cells with top 10 (i.e., 10/1091; 0.9%) PageRank values were extracted, covering 777 trajectories of 46 species (Table S2). Trajectories accounted for 88.5% (46/52) species and 55.1% (777/1410) trajectory sequences.

Independent data from 2020-2022 were used for model evaluation focusing on key stopover sites detection. The top 10 important cells covered 729 (729/1353; 53.9%) trajectories of 41 (41/52; 78.9%) species (Table S3). These important cells revealed that the sites during our three-year study period also stand out as important stopovers in the test years.

Also, we assessed the results of geographic functional similarity through the overlapped species for 2017-2019. The number of overlapped species revealed that the more species overlap, the higher the similarity is (Tables 2 and S2).

Table 2. Top 10 important stopovers and their potential alternative sites with overlapped species analysis for 2017-2019

Top 10 important stopovers (included species number)	Potential alternative stopover sites (overlapped species number)	
237(10)	236(8)	165(2)
589(25)	659(17)	624(17)
554(19)	519(13)	624(14)
520(9)	519(9)	485(6)
519(15)	520(9)	485(7)
952(13)	917(11)	987(10)
271(12)	237(9)	236(9)
624(19)	659(18)	694(17)
236(10)	235(3)	237(8)
918(20)	883(14)	952(13)

Table 3. Top 10 important stopovers and their potential alternative sites with overlapped species analysis for 2020-2022

Top 10 important stopovers (included species number)	Potential alternative stopover sites (overlapped species number)	
237(9)	236(7)	165(1)
589(20)	659(17)	624(18)
554(20)	519(15)	624(15)
520(14)	519(11)	485(7)
519(16)	520(13)	485(7)
952(11)	917(10)	987(10)
271(11)	237(9)	236(7)
624(19)	659(18)	694(15)
236(7)	235(3)	237(7)
918(18)	883(17)	952(10)

Data from 2020-2022 revealed the effectiveness of geo-functional similarity. That is, the similarity results revealed that the study period and the testing period share almost the same outcomes for potential alternative sites exploration (Tables 3 and S3).

Furthermore, Fig.8 showed different landcover classed in the three hotspots areas, including water, developed, barren/sparsely vegetated, tress, shrub and herbaceous with all the three areas having the most percentages of trees, where “CA” represented the Central America area, “FL” represented the Florida peninsula and its inland, and “PS” represented the region near Puget Sound. Fig 9 showed the HFP levels of the stopover hotspots: (1) PS: the distribution was concentrated at a low value with its median about 10, which indicated that human interference was relatively low and stable; (2) The Florida peninsula and its inland (FL): its median was about 17 with its maximum HFP value could be greater than 35, indicating that there was a rather strong human interference to parts of this area; (3) Central America (CA): its median was about 15 locating between FL and PS indicating moderate interference levels. Finally, the overlapping percentage between the stopover hotspot cells and IBAs was 13/18 (72.2%, grids in red and yellow) with 5/18 (27.8%) not identified as IBAs (Fig.10).

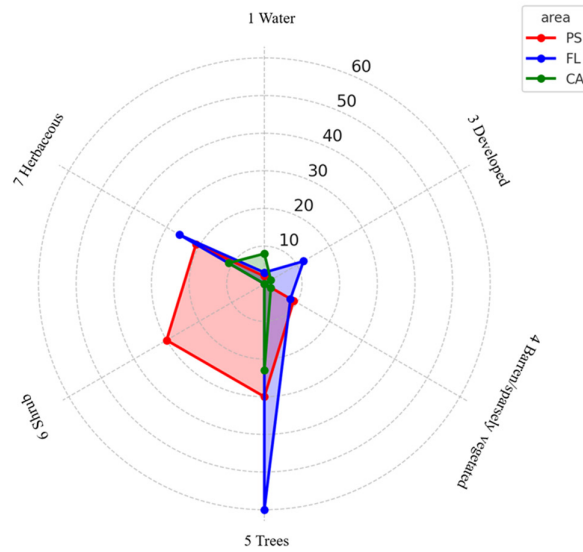


Figure 8. Landcover classes analysis with the GLanCE product. “CA” represents the Central America area, “FL” represents the Florida peninsula and its inland, and “PS” represents the region near Puget Sound. The figure above can show different landcover classes in the three hotspots areas, including water, developed, barren/sparsely vegetated, trees, shrub and herbaceous. And all the three areas have the most percentages of trees.

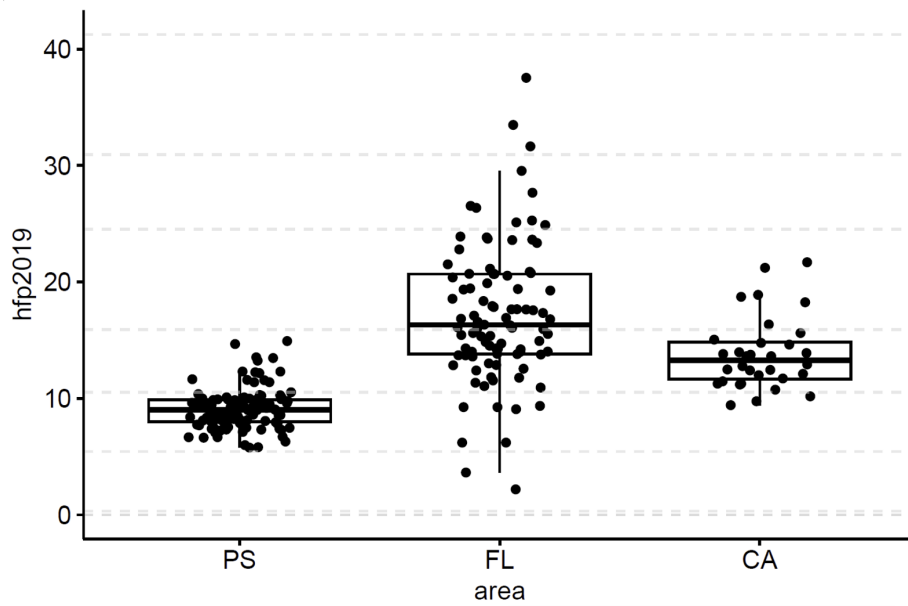


Figure 9. Human disturbance analysis with the Human Footprint dataset. The gray dotted lines represent the 0%, 1%, 5%, 25%, 50%, 75%, 95%, 99%, and 100% quantiles of the dataset which are 0.006, 0.316, 5.440, 10.511, 15.911, 24.520, 30.927, and 41.259 respectively. For the three stopover hotspots: (1) The region near Puget Sound (PS): the distribution is concentrated at a low value with its median about 10, which indicates that human interference is relatively low and stable; (2) The Florida peninsula and its inland (FL): its median is about 17 with its maximum HFP value can be greater than 35, indicating that there is a rather strong human interference to parts of this area; (3) Central America (CA): its median is about 15 locating between FL and PS indicating moderate interference levels.

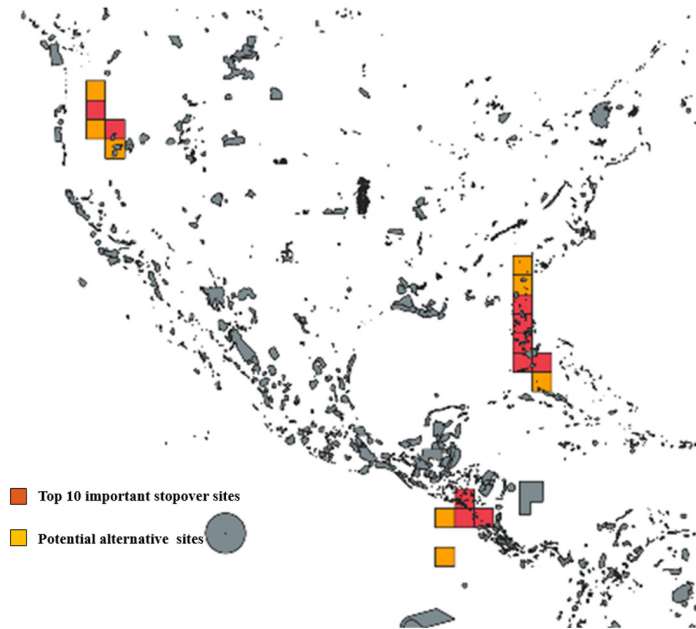


Figure 10. The stopover hotspots overlapped with the IBAs map. The overlapping percentage between the stopover hotspot cells and IBAs is 13/18 (72.2%, grids in red and yellow) with 5/18 (27.8%) not identified as IBAs.

DISCUSSION

This study combined the booming of public citizen science observation data with the urgent need to understand bird migration (Rosenberg et al., 2019). In this article, we presented a systematic method considering the network structure during migration for multi-species at the population level to help develop precision conservation strategies. Effective stopover hotspots mining and potential alternative sites exploration can help manage migration network connectivity and decrease migration risks, especially for long-distance migratory birds (Zurell et al., 2018). We applied the PageRank algorithm for stopover sites importance assessment considering both the linkage quantity and quality across the migration network for stopover hotspots discovery. We also explored the alternative sites for each hotspot based on geo-functional similarity using a word embedding technique. Our study effectively mined both the spatiotemporal and semantic information of the trajectory sequences and offered effective and prospective guidance for protection prioritization decisions. Our method employed 52 focal migratory species in North and Central America during 2017-2019, and generated rigorous estimations for stopover hotspots and potential alternative sites during migration.

Species analysis for stopover hotspots and their potential alternative sites

The larger number of species included in a stopover site can be used as a proxy of the high importance of the site. The more species overlapped between sites, the higher the similarity between the sites. That is to say, species sharing a stopover site could be a proxy of biogeographic analogy even in spatially disparate zones. And the species overlapped can indicate the similarity of geographic functions, which means areas attract more same species, the more similar their geographic functions is. We note that cell 237 acquires a higher PageRank value for its crucial location as the “bottleneck” of the American flyway. This area is around the Central American isthmus, includes plains and Central volcanic ridge covered with rich forests and some farmlands as well as both water and well-protected land resources, which can provide support and evidence for the inference of Central America’s significant value for migratory bird network connectivity (Bayly et al., 2018). Detection of relevant cells can give refined and scientific targets for Central America protection against potential threats from forest loss and expansion of land conversion (Cohen et al., 2007).

Stopover hotspots characteristics analysis

With the growing attention to migratory bird protection, there is a great need for informed protection of stopover hotspots across migratory paths. We found fundamental stopover sites across a migration network and potential alternative sites for further management accounting for human activity. Our finding mirrored other efforts for data-driven biodiversity conservation. Studies have explored relevant decision-making plans. For example, Thomson et al. (2020) developed a landscape-scale spatial conservation action planning tool (SCAP) to offer advances for conservation actions in heterogeneous landscapes. Guo et al. (2024) discussed the relationship between protection status and light pollution with the stopover hotspots distribution in the eastern US.

Migratory birds need water to drink and feed. Thus, areas close to water sources, such as coastlines, freshwater lakes, rivers, and wetlands, are often crucial stopovers (Boere et al., 2006). Different species of migratory birds have different habitat needs. Thus, heterogeneous habitats can attract more migratory species (Tu et al., 2020). The three stopover hotspot areas (FL, CA, and the region near PS) were found close to water sources and food sources like forests. The stopover sites CA and PS are currently surrounded by terrestrial and marine protected areas. The regions around FL, however, are not under sufficient protection. Considering the high-level population density and economic development (Mu et al., 2022), it may be necessary to involve proper urban development planning and private lands involvement for improved stopover protection in the eastern US. Results highlighted the importance of forest conservation for bird migration (Guo et al., 2023; Mehlman et al., 2005).

Also, the land cover of CA, FL and the region near PS is dominated by trees, calling for more attention while making bird conservation decisions (Fig.8). HFP index levels of the region near PS suggest a lower level of human disturbance. CA shows moderate but widespread human presence. In contrast, FL shows a wide range of HFP values, with many cells experiencing high levels of anthropogenic impact, which needs more protection activities (Fig.9).

Lastly, the three hotspot areas overlap with the protected areas in North and Central America (Fig.10, 72.2% overlap). McClure et al. (2018) suggested enhancing cooperation through policy mechanisms that account for protected areas for raptor species along the Central America area. Kirby et al. (2008) called for attention to agricultural intensification, human infrastructure development, and forest protection based on protected areas for migratory landbird and waterbird species. It is unclear whether birds

select migration stopovers in protected areas or if protected areas are established in sites recognized as important for seasonal bird congregation.

Future directions

One important limitation of our work is the limited capacity to detect areas with small PageRank values that are still relevant to migration connectivity. For example, some endangered species could have low eBird records resulting in weak signal of stopover hotspots, but could be the species in higher need of management and protection, such as Kirtland's Warbler (*Setophaga kirtlandii*) breeding in the Great Lakes. Areas not covered by eBird observations are not assessed and, instead, oversampled areas provide more information at the cost of bias. Assisting with individual tracking data, human movement data or other observation datasets (Ai et al., 2024) could complement our stopover hotspots map. Additionally, PageRank algorithm and word embedding technique only consider the link relationship between nodes, and ignored other information, such as human and bird behavioral data. Finally, eBird data has the biases and limitations that citizen science data have, such as the bias from regional differences in reporting rates that depend heavily on species' overlap with eBird users' activities (Robinson et al., 2022). To address this data limitation, information from different databases and additional taxa during longer periods would help detect and mitigate systematic bias from a single data platform.

CONCLUSION

Our novel analytical approach to access migratory patterns revealed important stopover nodes in the migratory network for a comprehensive range of bird taxa in North and Central America. We extracted important stopover signals based on the network-level evaluation method by PageRank algorithm, and explored alternative stopover sites that accounted for spatial and temporal context information of trajectory sequences between sites with word embeddings, avoiding studying the sites as isolated ones. Targeted protection and recharging of areas near water and forests were recommended in the sites identified as hot stopover sites of bird migration, especially in developed land in the eastern United States. Discoveries and analytical approaches presented here could be useful for migratory connectivity protection in the full migration cycle and inform multinational conservation prioritization.

DATA AND CODE AVAILABILITY

Data and code used to perform this study are available at GitHub (<https://github.com/ash0920-git/stopover-hotspots>).

ACKNOWLEDGEMENTS

This work is supported by the National Key R&D Program of China (2022YFF0802300), National Natural Science Foundation of China (U21A20478), Zhejiang High-Level Talents Special Support Program (2021R52002). LEE was supported by National Science Foundation CAREER (2235295) and HEGS (2116748) awards, NIH K01AI168452 award, Virginia Tech DA PPP, CeZAP, and ICTAS grants, and the Chinese Academy of Sciences PIFI project 2024PVC0085. The content is solely the responsibility of the authors and does not necessarily represent the official views of the National Institutes of Health.

COMPETING INTERESTS

The authors have declared that no competing interests exist.

REFERENCES

- Ai, Y., Zhai, H., Sun, Z., Yan, W., and Hu, T., 2024. Flock-Seer: a portable stereo vision observer for bird flocking. *IET Cyber Syst. Robot.* 6(1): e12118. <https://doi.org/10.1049/csy2.12118>
- Artificial light map, 2024. <https://www.nasachina.cn/apod/19232.html> (accessed June 14, 2024)
- Bayly, N. J., Rosenberg, K. V., Easton, W. E., Gomez, C., Carlisle, J. A. Y., Ewert, D. N., and Goodrich, L., 2018. Major stopover regions and migratory bottlenecks for Nearctic-Neotropical landbirds within the Neotropics: a review. *Bird Conserv. Int.* 28(1): 1-26. <https://doi.org/10.1017/S0959270917000296>
- Berger, M., McDonough, K., and Seversky, L. M., 2016. cite2vec: citation-driven document exploration via word embeddings. *IEEE Trans. Vis. Comput. Graph.* 23(1): 691-700. <https://doi.org/10.1109/TVCG.2016.2598667>
- Boere, G. C., Galbraith, C. A., and Stroud, D. A. (Eds.), 2006. *Waterbirds around the world: a global overview of the conservation, management and research of the world's waterbird flyways*.
- Bonter, D. N., Gauthreaux Jr, S. A., and Donovan, T. M., 2009. Characteristics of important stopover locations for migrating birds: remote sensing with radar in the Great Lakes Basin. *Conserv. Biol.* 23(2): 440-448. <https://doi.org/10.1111/j.1523-1739.2008.01085.x>
- Catry, T., Correia, E., Gutiérrez, J. S., Bocher, P., Robin, F., Rousseau, P., and Granadeiro, J. P., 2024. Low migratory connectivity and similar migratory strategies in a shorebird with contrasting wintering population trends in Europe and West Africa. *Sci. Rep.* 14(1): 4884. <https://doi.org/10.1038/s41598-024-55501-y>
- Cohen, E. B., Barrow Jr, W. C., Buler, J. J., Deppe, J. L., Farnsworth, A., Marra, P. P., and Moore, F. R., 2017. How do en route events around the Gulf of Mexico influence migratory landbird populations? *Condor Ornithol. Appl.* 119(2): 327-343. <https://doi.org/10.1650/CONDOR-17-20.1>
- Derpanis, K. G., 2005. Mean-Shift clustering. Lecture Notes. [Online]. Available: http://www.cse.yorku.ca/%7Ekosta/CompVis_Notes/mean_shift.pdf (accessed 10 March 2023)
- Donald, P. F., Fishpool, L. D., Ajagbe, A., Bennun, L. A., Bunting, G., Burfield, I. J., ... and Wege, D. C., 2019. Important Bird and Biodiversity Areas (IBAs): the development and characteristics of a global inventory of key sites for biodiversity. *Bird Conserv. Int.* 29(2), 177-198. <https://doi.org/10.1017/S0959270918000102>
- eBird, 2023. <https://ebird.org/> (accessed April 22, 2023)
- Feng, S., Yang, Q., Hughes, A. C., Chen, J., and Qiao, H., 2021. A novel method for multi-trajectory reconstruction based on LoMcT for avian migration in population level. *Eco. Inform.* 63: 101319. <https://doi.org/10.1016/j.ecoinf.2021.101319>
- Gazoni, E. and Clark, C, 2023. openpyxl 3.1.2. Available from: <https://pypi.org/project/openpyxl/> (accessed 10 Feb 2024)
- GBIF. Available from <https://www.gbif.org/> (accessed 20 August 2023)
- Grisel, O., Mueller, A., ... and Eren, K., 2022. scikit-learn/scikit-learn: scikit-learn 1.1.2. Available from: <https://zenodo.org/records/6968622> (accessed 10 Feb 2023)
- Guo, F., Buler, J. J., Smolinsky, J. A., and Wilcove, D. S., 2023. Autumn stopover hotspots and multi-scale habitat associations of migratory landbirds in the eastern United States. *Proc. Natl. Acad. Sci.* 120(13): e2203511120. <https://doi.org/10.1073/pnas.2203511120>
- Guo, F., Buler, J. J., Smolinsky, J. A., and Wilcove, D. S., 2024. Seasonal patterns and protection status of stopover hotspots for migratory landbirds in the eastern United States. *Curr. Biol.* 34(1): 235-244. <https://doi.org/10.1016/j.cub.2023.11.033>
- Harris, C.R., Millman, K.J., van der Walt, S.J. et al., 2020. Array programming with NumPy. *Nature* 585, 357–362. <https://doi.org/10.1038/s41586-020-2649-2>
- Hastie, T. J., and Tibshirani, R. J., 1990. *Generalized Additive Models* (Vol. 43). CRC Press, London.
- Higuchi, H., 2012. Bird migration and the conservation of the global environment. *J. Ornithol.* 153(Suppl 1), 3-14. <https://doi.org/10.1007/s10336-011-0768-0>

- Hong, L., Qian, Y., Gong, C., Zhang, Y., and Zhou, X., 2023. Improved Key Node Recognition Method of Social Network Based on PageRank Algorithm. *Comput. Mater. Continua*. 74(1). <https://doi.org/10.32604/cmc.2023.029180>
- Hunter, J.D. 2007. Matplotlib: a 2D Graphics Environment. *Comput. Sci. Eng.* 9 (3), 90-95. <https://doi.org/10.1109/MCSE.2007.55>
- Jin, Y. T., You, J., Wakamiya, S., and Kwon, H. Y., 2024. Analyzing user reactions using relevance between location information of tweets and news articles. *EPJ Data Sci.* 13(1): 44. <https://doi.org/10.1140/epjds/s13688-024-00465-2>
- Kaiser, A., 1999. Stopover strategies in birds: a review of methods for estimating stopover length. *Bird Study*. 46 (Supplement): S299-S308. <https://doi.org/10.1080/00063659909477257>
- Kirby, J. S., Stattersfield, A. J., Butchart, S. H., Evans, M. I., Grimmett, R. F., Jones, V. R., ... and Newton, I., 2008. Key conservation issues for migratory land- and waterbird species on the world's major flyways. *Bird Conserv. Int.*, 18(S1), S49-S73. <https://doi.org/10.1017/S0959270908000439>
- Knight, S. M., Bradley, D. W., Clark, R. G., Gow, E. A., Bélisle, M., Berzins, L. L., ...and Norris, D. R., 2018. Constructing and evaluating a continent-wide migratory songbird network across the annual cycle. *Ecol. Monogr.* 88(3): 445-460. <https://doi.org/10.1002/ecm.1298>
- Kramer, G. R., Andersen, D. E., Buehler, D. A., Wood, P. B., Peterson, S. M., Lehman, J. A., ... and Streby, H. M., 2018. Population trends in *Vermivora* warblers are linked to strong migratory connectivity. *Proc. Natl. Acad. Sci.* 115(14): E3192-E3200. <https://doi.org/10.1073/pnas.1718985115>
- La Sorte, F. A., Fink, D., Hochachka, W. M., and Kelling, S., 2016. Convergence of broad-scale migration strategies in terrestrial birds. *Proc. R. Soc. B.* 283(1823): 20152588. <https://doi.org/10.1098/rspb.2015.2588>
- Levy, O., and Goldberg, Y., 2014. Dependency-based word embeddings. *Proc. 52nd Annu. Meet. Assoc. Comput. Linguist.* <https://doi.org/10.3115/v1/P14-2050>
- Lin, H. Y., Schuster, R., Wilson, S., Cooke, S. J., Rodewald, A. D., and Bennett, J. R., 2020. Integrating season-specific needs of migratory and resident birds in conservation planning. *Biol. Conserv.* 252: 108826. <https://doi.org/10.1016/j.biocon.2020.108826>
- Liu, F., Zheng, L., and Zheng, J., 2020. HieNN-DWE: a hierarchical neural network with dynamic word embeddings for document-level sentiment classification. *Neurocomputing*. 403: 21-32. <https://doi.org/10.1016/j.neucom.2020.04.084>
- Machin, J., 2017. xlwt 1.3.0. Available from: <https://pypi.org/project/xlwt/> (accessed 12 Feb 2022)
- Marín, S. D., 2018. pygam 0.8.0. Available from: <https://pypi.org/project/pygam/> (accessed 11 Feb 2022)
- MATLAB, R2021b. version 9.11.0.1873467, Natick, Massachusetts: The MathWorks Inc.
- McClure, C. J., Westrip, J. R., Johnson, J. A., Schulwitz, S. E., Virani, M. Z., Davies, R., ... and Butchart, S. H., 2018. State of the world's raptors: Distributions, threats, and conservation recommendations. *Biol. Conserv.*, 227, 390-402. <https://doi.org/10.1016/j.biocon.2018.08.012>
- McCormick, C., 2016. Word2vec tutorial-the skip-gram model. [Online]. Available: <http://mccormickml.com/2016/04/19/word2vec-tutorial-the-skip-gram-model>
- Mehlman, D. W., Mabey, S. E., Ewert, D. N., Duncan, C., Abel, B., Cimprich, D., ... and Woodrey, M., 2005. Conserving stopover sites for forest-dwelling migratory landbirds. *The Auk*, 122(4), 1281-1290. <https://doi.org/10.1093/auk/122.4.1281>
- Mikolov, T., Chen, K., Corrado, G., and Dean, J., 2013. Efficient estimation of word representations in vector space. *arXiv preprint arXiv:1301.3781*. <https://doi.org/10.48550/arXiv.1301.3781>
- Mikolov, T., Sutskever, I., Chen, K., Corrado, G. S., and Dean, J., 2013. Distributed representations of words and phrases and their compositionality. *NeurIPS*. 26. <https://doi.org/10.48550/arXiv.1310.4546>
- Mu, H., Li, X., Wen, Y., Huang, J., Du, P., Su, W., ... and Geng, M., 2022. A global record of annual terrestrial Human Footprint dataset from 2000 to 2018. *Sci. Data*, 9(1), 176. <https://doi.org/10.1038/s41597-022-01284-8>
- Nemes, C. E., Cabrera-Cruz, S. A., Anderson, M. J., DeGroot, L. W., DeSimone, J. G., Massa, M. L., and Cohen, E. B., 2023. More than mortality: consequences of human activity on migrating birds extend beyond direct mortality. *Ornithol. Appl.* 125(3), duad020. <https://doi.org/10.1093/ornithapp/duad020>
- Nicol, S., Cros, M. J., Peyrard, N., Sabbadin, R., Trépos, R., Fuller, R. A., and Woodworth, B. K., 2023. FlywayNet: a hidden semi-Markov model for inferring the structure of migratory bird networks from count data. *Methods Ecol. Evol.* 14(2): 265-279. <https://doi.org/10.1111/2041-210X.14011>
- Page, L., Brin, S., Motwani, R., and Winograd, T., 1999. The PageRank citation ranking: bringing order to the web. *Stanford Infolab*. [Online]. Available: <http://ilpubs.stanford.edu:8090/422/1/1999-66.pdf>
- Python 3.10. Python Software Foundation, 2021.

- Qian, M., Liu, J., Li, C., and Pals, L., 2019. A comparative study of English-Chinese translations of court texts by machine and human translators and the Word2Vec based similarity measure's ability to gauge human evaluation biases. *Proc. MT Summit XVII: Translator, Project and User Tracks*. pp: 95-100. <https://aclanthology.org/W19-6714.pdf>
- Reback, J., Jbrockmendel, McKinney, W., van Den Bossche, J., Roeschke, M., ... and Augspurger, T. *pandas dev/pandas: Pandas1.4.3*. Available from: <https://zenodo.org/record/3509134> (accessed 2 Feb 2023)
- Rehurek, R., 2023. *gensim 4.3.1*. Available from: <https://pypi.org/project/gensim/> (accessed 2 Feb 2024)
- Robinson, O. J., Socolar, J. B., Stuber, E. F., Auer, T., Berryman, A. J., Boersch-Supan, P. H., ... and Johnston, A., 2022. Extreme uncertainty and unquantifiable bias do not inform population sizes. *Proc. Natl. Acad. Sci.* 119(10): e2113862119. <https://doi.org/10.1073/pnas.2113862119>
- Rogers, I., 2002. The Google Pagerank algorithm and how it works. [Online]. Available: https://cs.wmich.edu/gupta/teaching/cs3310/lectureNotes_cs3310/Pageran%20Explained%20Correctly%20with%20Examples_www.cs.princeton.ed~chazelle_courses_BIB_pagerank.pdf
- Rosenberg, K. V., Dokter, A. M., Blancher, P. J., Sauer, J. R., Smith, A. C., Smith, P. A., and Marra, P. P., 2019. Decline of the North American avifauna. *Science*, 366(6461):120-124. <https://doi.org/10.1126/science.aaw1313>
- Runge, C. A., Watson, J. E., Butchart, S. H., Hanson, J. O., Possingham, H. P., and Fuller, R. A., 2015. Protected areas and global conservation of migratory birds. *Science*, 350(6265): 1255-1258. <https://doi.org/10.1126/science.aac9180>
- Schrimpf, M. B., Des Brisay, P. G., Johnston, A., Smith, A. C., Sánchez-Jasso, J., Robinson, B. G., and Koper, N., 2021. Reduced human activity during COVID-19 alters avian land use across North America. *Sci. Adv.* 7(2): eabf5073. <https://doi.org/10.1126/sciadv.abf5073>
- Somveille, M., Bay, R. A., Smith, T. B., Marra, P. P., and Ruegg, K. C., 2021. A general theory of avian migratory connectivity. *Ecol. Lett.* 24(9): 1848-1858. <https://doi.org/10.1111/ele.13817>
- Stanimirova, R., Tarrio, K., Turlej, K., McAvoy, K., Stonebrook, S., Hu, K. T., ... and Friedl, M. A., 2023. A global land cover training dataset from 1984 to 2020. *Sci. Data*, 10(1), 879. <https://doi.org/10.1038/s41597-023-02798-5>
- Thomson, J., Regan, T. J., Hollings, T., Amos, N., Geary, W. L., Parkes, D., ... and White, M., 2020. Spatial conservation action planning in heterogeneous landscapes. *Biol. Conserv.* 250, 108735. <https://doi.org/10.1016/j.biocon.2020.108735>
- Tu, H. M., Fan, M. W., and Ko, J. C. J., 2020. Different habitat types affect bird richness and evenness. *Sci. Rep.*, 10(1), 1221. <https://doi.org/10.1038/s41598-020-58202-4>
- USGS geographic map, 2024. <https://apps.nationalmap.gov/viewer/> (accessed June 17, 2024)
- Wang, H., Hernandez, J. M., and van Mieghem, P., 2008. Betweenness centrality in a weighted network. *Phys. Rev. E Stat. Nonlin. Soft Matter Phys.*, 77(4), 046105. <https://doi.org/10.1103/PhysRevE.77.046105>
- Wang, M., Yang, S., Sun, Y., and Gao, J., 2017. Discovering urban mobility patterns with PageRank based traffic modeling and prediction. *Physica A: Stat. Mech. Appl.* 485: 23-34. <https://doi.org/10.1016/j.physa.2017.04.155>
- Webster, M. S., Marra, P. P., Haig, S. M., Bensch, S., and Holmes, R. T., 2002. Links between worlds: unraveling migratory connectivity. *Trends Ecol. Evol.* 17(2), 76-83. [https://doi.org/10.1016/S0169-5347\(01\)02380-1](https://doi.org/10.1016/S0169-5347(01)02380-1)
- Whitaker, J., 2022. *basemap 1.3.4*. Available from: <https://pypi.org/project/basemap/> (accessed 3 Feb 2023)
- Whitaker, J., 2022. *pyproj 3.3.1*. Available from: <https://zenodo.org/record/3509134> (accessed 7 Feb 2023)
- Withers, C., 2020. *xldr 2.0.1*. Available from: <https://pypi.org/project/basemap/> (accessed 13 Feb 2022)
- World Database on Protected Areas, 2024. <https://www.protectedplanet.net/en/thematic-areas/wdpa?tab=WDPA> (accessed May 15, 2024)
- Wyborn, C., and Evans, M. C., 2021. Conservation needs to break free from global priority mapping. *Nat. Ecol. Evol.* 5(10): 1322-1324. <https://doi.org/10.1038/s41559-021-01540-x>
- Xiong, S., Lv, H., Zhao, W., and Ji, D., 2018. Towards Twitter sentiment classification by multi-level sentiment-enriched word embeddings. *Neurocomputing*, 275:2459-2466. <https://doi.org/10.1016/j.neucom.2017.11.023>
- Xu, Y., Si, Y., Takekawa, J., Liu, Q., Prins, H. H., Yin, S., ... and de Boer, W. F., 2020. A network approach to prioritize conservation efforts for migratory birds. *Conserv. Biol.* 34(2): 416-426. <https://doi.org/10.1111/cobi.13383>
- Yorav-Raphael, N. and da Costa-Luis, C., 2024. Tqdm: a fast, extensible progress bar for python and cli, <https://github.com/tqdm/tqdm>, Version 4.65.0.

- Zhang, T. Y., and Wang, X. L., 2011. Outlier detection algorithm based on space local deviation factor. *Comput. Eng.* 14. <https://doi.org/10.3969/j.issn.1000-3428.2011.14.096> (in Chinese with English abstract)
- Zhang, W., Wei, J., and Xu, Y., 2023. Prioritizing global conservation of migratory birds over their migration network. *One Earth*, 6(11): 1340-1349. <https://doi.org/10.1016/j.oneear.2023.08.017>
- Zhu, M., Chen, W., Xia, J., Ma, Y., Zhang, Y., Luo, Y., and Liu, L., 2019. Location2vec: a situation-aware representation for visual exploration of urban locations. *IEEE Trans. Intell. Transp. Syst.* 20(10): 3981-3990. <https://doi.org/10.1109/TITS.2019.2901117>
- Zivot, E., and Wang, J., 2007. Modeling financial time series with S-Plus® (Vol. 191). Springer Science & Business Media.
- Zumstein,F.,2023. xlwings 0.30.6. Available from: <https://pypi.org/project/xlwings/> (accessed 13 Feb 2024)
- Zurell, D., Graham, C. H., Gallien, L., Thuiller, W., and Zimmermann, N. E., 2018. Long-distance migratory birds threatened by multiple independent risks from global change. *Nat. Clim. Chang.* 8(11): 992-996. <https://doi.org/10.1038/s41558-018-0312-9>

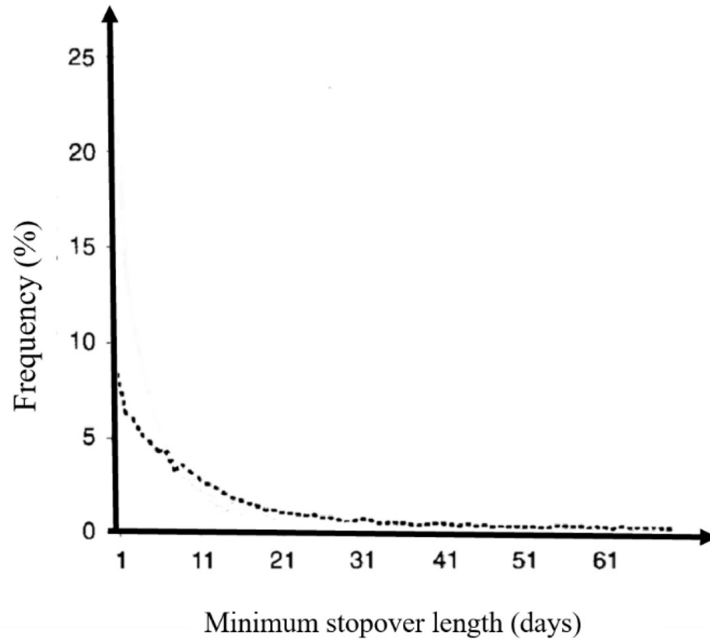
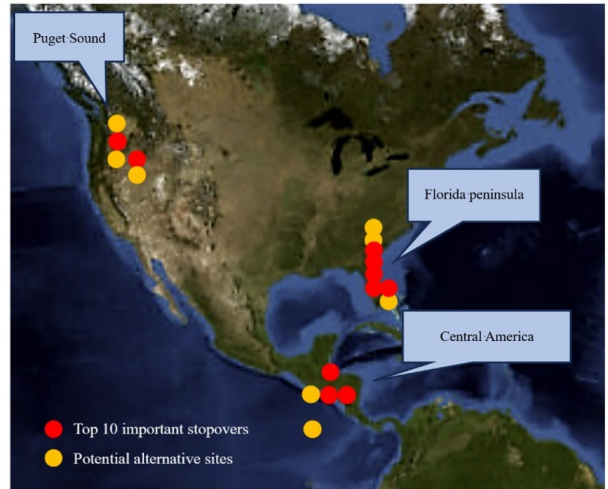


Figure S1. Frequency distribution of minimum stopover length during autumn migration periods



(a) Stopover hotspots overlapped with the artificial light map



(b) Stopover hotspots overlapped with the topographic map

Figure S2. Stopover hotspots overlapped with the artificial light map and topographic map

Table S1. Species list and their habitats information*

Number	Species name
1	<i>Accipiter cooperii</i> Breeds in forested areas; more common in suburban areas.
2	<i>Aix sponsa</i> Found in wetlands and flooded woods.
3	<i>Anas platyrhynchos</i> Found anywhere with water, including city parks, backyard creeks, and various wetland habitats.
4	<i>Archilochus colubris</i> Readily comes to sugar water feeders and flower gardens.
5	<i>Ardea alba</i> Ponds, marshes, and tidal mudflats.
6	<i>Ardea Herodias</i> Occurs in almost any wetland habitat, from small ponds to marshes to saltwater bays.
7	<i>Branta canadensis</i> Occurs in any open or wetland habitat.
8	<i>Bucephala albeola</i> Found in bays, estuaries, reservoirs, and lakes in winter. Travels to boreal forest and nests in cavities in summer.
9	<i>Buteo jamaicensis</i> Edges of trees.
10	<i>Buteo lineatus</i> Often in forested areas.
11	<i>Catharus ustulatus</i> Breeds in the boreal forest.
12	<i>Charadrius vociferus</i> Often in fields with short grass or barren dirt.
13	<i>Colaptes auratus</i> Often seen feeding on the ground in open areas, foraging for ants and worms.
14	<i>Cyanocitta cristata</i> Pairs or small groups travel through mature deciduous or coniferous woodlands.
15	<i>Dumetella carolinensis</i> Especially thickets or second-growth at the edge of forests, often near water.
16	<i>Egretta thula</i> Found in a variety of wetland habitats, especially shallow marshy pools and mudflats.
17	<i>Fulica americana</i> Ponds, city parks, marshes, reservoirs, lakes, ditches, and saltmarshes.
18	<i>Geothlypis trichas</i> Found in shrubby wet areas, including marshes, forest edges, and fields.
19	<i>Haliaeetus leucocephalus</i> Near bodies of water.
20	<i>Hirundo rustica</i> Especially large fields and wetlands.
21	<i>Icterus galbula</i> Breeds in deciduous trees in open woodlands, forest edges, orchards, riversides, parks, and backyards.
22	<i>Larus delawarensis</i> Found along lakes, rivers, ponds, and beaches.
23	<i>Leiostyris celata</i> Found in scrubby areas, woodland edge, and thickets.

Number	Species name
24	<i>Leiothlypis ruficapilla</i> Breeds in coniferous or mixed forests.
25	<i>Mareca strepera</i> Typically found in pairs or small flocks in shallow wetlands, ponds, or bays.
26	<i>Megasceryle alcyon</i> Edges of streams, lakes, and estuaries.
27	<i>Melospiza melodia</i> Especially edges of fields, often near water.
28	<i>Molothrus aterwoods</i> Farmland, and stockyards.
29	<i>Myiarchus crinitus</i> Deciduous forests.
30	<i>Pandion haliaetus</i> On top of channel markers, utility poles and high platforms near water.
31	<i>Passerina cyaneathe</i> Edge of forests and fields.
32	<i>Pheucticus ludovicianus</i> Especially in deciduous forests.
33	<i>Pipilo erythrophthalmus</i> Inhabits scrubby areas and forest edges.
34	<i>Podilymbus podiceps</i> Occurs on ponds and marshes.
35	<i>Poliophtila caerulea</i> Breed in deciduous woodlands, often near water.
36	<i>Quiscalus quiscula</i> Forages in fields, scrubby areas, and open woods.
37	<i>Sayornis phoebe</i> Woodland edge, brushy fields, or edges of ponds.
38	<i>Setophaga americana</i> Breeds in mature coniferous or deciduous forests, especially near water.
39	<i>Setophaga coronata</i> Mixed forests, often near clearings or edges. In migration and winter, found in any woodland or open shrubby area, including coastal dunes, fields, parks, and residential areas.
40	<i>Setophaga palmarum</i> Breeds in bogs and clearings in the boreal forest.
41	<i>Setophaga petechia</i> Near water, often foraging in shrubs fairly low to the ground.
42	<i>Sialia sialis</i> Favors fields and open woods.
43	<i>Spatula discors</i> Usually found in shallow wetlands or marshes.
44	<i>Spinus tristis</i> Found in weedy fields, cultivated areas, roadsides, orchards, and backyards.
45	<i>Spizella passerina</i> Usually found in open woodlands, scrubby areas, or even in suburban settings.
46	<i>Stelgidopteryx serripennis</i> Often seen near water, sometimes in mixed flocks with other swallows.

Number	Species name
47	<i>Sturnus vulgaris</i> Often abundant, gathering in large flocks in open agricultural areas and towns and cities.
48	<i>Toxostoma rufum</i> Shrubby habitats, especially second-growth woodland, thickets, and forest edge.
49	<i>Troglodytes aedon</i> Open or semiopen habitats, including suburbs, parks, rural farmland, and woodland edge with thick tangles.
50	<i>Turdus migratorius</i> In gardens, parks, yards, golf courses, fields, pastures, and many other wooded habitats.
51	<i>Zenaida macroura</i> Found in a variety of habitats from agricultural fields to lightly wooded areas.
52	<i>Zonotrichia leucophrys</i> Breeds in brushy areas or thickets in open forest, often with conifers.

*The habitat information is collected from eBird (<https://ebird.org/>).

Table S2. Cell-IDs with the included species for 2017-2019

Top 10 important stopovers		Potential alternative stopover sites			
Cell-ID	Species	Cell-ID	Species	Cell-ID	Species
237	<i>Catharus ustulatus</i>	236	<i>Catharus ustulatus</i>	165	<i>Pheucticus ludovicianus</i>
	<i>Egretta thula</i>		<i>Hirundo rustica</i>		<i>Setophaga petechia</i>
	<i>Hirundo rustica</i>		<i>Myiarchus crinitus</i>		
	<i>Myiarchus crinitus</i>		<i>Pandion haliaetus</i>		
	<i>Pandion haliaetus</i>		<i>Pheucticus ludovicianus</i>		
	<i>Pheucticus ludovicianus</i>		<i>Setophaga petechia</i>		
	<i>Setophaga petechia</i>		<i>Sialia sialis</i>		
	<i>Sialia sialis</i>		<i>Spatula discors</i>		
	<i>Spatula discors</i>		<i>Troglodytes aedon</i>		
	<i>Ardea alba</i>		<i>Icterus galbula</i>		
589	<i>Archilochus colubris</i>	659	<i>Buteo lineatus</i>	624	<i>Buteo jamaicensis</i>
	<i>Ardea alba</i>		<i>Geothlypis trichas</i>		<i>Buteo lineatus</i>
	<i>Buteo jamaicensis</i>		<i>Icterus galbula</i>		<i>Geothlypis trichas</i>
	<i>Dumetella carolinensis</i>		<i>Myiarchus crinitus</i>		<i>Leiothlypis ruficapilla</i>
	<i>Egretta thula</i>		<i>Pandion haliaetus</i>		<i>Myiarchus crinitus</i>
	<i>Geothlypis trichas</i>		<i>Poliophtila caerulea</i>		<i>Pandion haliaetus</i>
	<i>Leiothlypis ruficapilla</i>		<i>Sayornis phoebe</i>		<i>Pheucticus ludovicianus</i>
	<i>Myiarchus crinitus</i>		<i>Setophaga americana</i>		<i>Podilymbus podiceps</i>
	<i>Pandion haliaetus</i>		<i>Setophaga coronata</i>		<i>Poliophtila caerulea</i>
	<i>Passerina cyanea</i>		<i>Setophaga palmarum</i>		<i>Sayornis phoebe</i>
	<i>Pheucticus ludovicianus</i>		<i>Dumetella carolinensis</i>		<i>Setophaga americana</i>
	<i>Podilymbus podiceps</i>		<i>Podilymbus podiceps</i>		<i>Setophaga palmarum</i>
	<i>Poliophtila caerulea</i>		<i>Quiscalus quiscula</i>		<i>Stelgidopteryx serripennis</i>
	<i>Quiscalus quiscula</i>		<i>Stelgidopteryx serripennis</i>		<i>Dumetella carolinensis</i>
	<i>Sayornis phoebe</i>		<i>Buteo jamaicensis</i>		<i>Icterus galbula</i>
	<i>Setophaga americana</i>		<i>Catharus ustulatus</i>		<i>Spatula discors</i>
	<i>Setophaga palmarum</i>		<i>Hirundo rustica</i>		<i>Catharus ustulatus</i>
	<i>Spatula discors</i>		<i>Leiothlypis ruficapilla</i>		<i>Hirundo rustica</i>
	<i>Stelgidopteryx serripennis</i>		<i>Megasceryle alcyon</i>		<i>Quiscalus quiscula</i>
	<i>Bucephala albeola</i>		<i>Pheucticus ludovicianus</i>		
	<i>Catharus ustulatus</i>		<i>Spizella passerina</i>		
	<i>Charadrius vociferus</i>				
	<i>Icterus galbula</i>				
	<i>Hirundo rustica</i>				
	<i>Setophaga petechia</i>				
554	<i>Archilochus colubris</i>	519	<i>Buteo jamaicensis</i>	624	<i>Buteo jamaicensis</i>
	<i>Buteo jamaicensis</i>		<i>Fulica americana</i>		<i>Buteo lineatus</i>
	<i>Dumetella carolinensis</i>		<i>Myiarchus crinitus</i>		<i>Geothlypis trichas</i>
	<i>Egretta thula</i>		<i>Pandion haliaetus</i>		<i>Leiothlypis ruficapilla</i>
	<i>Geothlypis trichas</i>		<i>Passerina cyanea</i>		<i>Myiarchus crinitus</i>
	<i>Myiarchus crinitus</i>		<i>Podilymbus podiceps</i>		<i>Pandion haliaetus</i>
	<i>Pandion haliaetus</i>		<i>Setophaga americana</i>		<i>Pheucticus ludovicianus</i>
	<i>Passerina cyanea</i>		<i>Setophaga palmarum</i>		<i>Podilymbus podiceps</i>
	<i>Pheucticus ludovicianus</i>		<i>Catharus ustulatus</i>		<i>Poliophtila caerulea</i>
	<i>Podilymbus podiceps</i>		<i>Egretta thula</i>		<i>Sayornis phoebe</i>
	<i>Poliophtila caerulea</i>		<i>Leiothlypis ruficapilla</i>		<i>Setophaga americana</i>
	<i>Setophaga americana</i>		<i>Pheucticus ludovicianus</i>		<i>Setophaga palmarum</i>
	<i>Setophaga palmarum</i>		<i>Stelgidopteryx serripennis</i>		<i>Stelgidopteryx serripennis</i>
	<i>Anas platyrhynchos</i>		<i>Hirundo rustica</i>		<i>Dumetella carolinensis</i>
	<i>Catharus ustulatus</i>		<i>Setophaga petechia</i>		<i>Icterus galbula</i>
	<i>Leiothlypis ruficapilla</i>				<i>Spatula discors</i>
	<i>Hirundo rustica</i>				<i>Catharus ustulatus</i>
	<i>Setophaga petechia</i>				<i>Hirundo rustica</i>
	<i>Spatula discors</i>				<i>Quiscalus quiscula</i>

Top 10 important stopovers		Potential alternative stopover sites			
Cell-ID	Species	Cell-ID	Species	Cell-ID	Species
520	<i>Myiarchus crinitus</i>	519	<i>Buteo jamaicensis</i>	485	<i>Buteo jamaicensis</i>
	<i>Pandion haliaetus</i>		<i>Fulica americana</i>		<i>Passerina cyanea</i>
	<i>Passerina cyanea</i>		<i>Myiarchus crinitus</i>		<i>Podilymbus podiceps</i>
	<i>Podilymbus podiceps</i>		<i>Pandion haliaetus</i>		<i>Setophaga americana</i>
	<i>Setophaga americana</i>		<i>Passerina cyanea</i>		<i>Myiarchus crinitus</i>
	<i>Setophaga palmarum</i>		<i>Podilymbus podiceps</i>		<i>Pheucticus ludovicianus</i>
	<i>Leiothlypis ruficapilla</i>		<i>Setophaga americana</i>		<i>Setophaga palmarum</i>
	<i>Pheucticus ludovicianus</i>		<i>Setophaga palmarum</i>		
	<i>Setophaga petechia</i>		<i>Catharus ustulatus</i>		
			<i>Egretta thula</i>		
519	<i>Buteo jamaicensis</i>	520	<i>Myiarchus crinitus</i>	485	<i>Buteo jamaicensis</i>
	<i>Fulica americana</i>		<i>Pandion haliaetus</i>		<i>Passerina cyanea</i>
	<i>Myiarchus crinitus</i>		<i>Passerina cyanea</i>		<i>Podilymbus podiceps</i>
	<i>Pandion haliaetus</i>		<i>Podilymbus podiceps</i>		<i>Setophaga americana</i>
	<i>Passerina cyanea</i>		<i>Setophaga americana</i>		<i>Myiarchus crinitus</i>
	<i>Podilymbus podiceps</i>		<i>Setophaga palmarum</i>		<i>Pheucticus ludovicianus</i>
	<i>Setophaga americana</i>		<i>Leiothlypis ruficapilla</i>		<i>Setophaga palmarum</i>
	<i>Setophaga palmarum</i>		<i>Pheucticus ludovicianus</i>		
	<i>Catharus ustulatus</i>		<i>Setophaga petechia</i>		
	<i>Egretta thula</i>				
952	<i>Aix sponsa</i>	917	<i>Anas platyrhynchos</i>	987	<i>Aix sponsa</i>
	<i>Anas platyrhynchos</i>		<i>Bucephala albeola</i>		<i>Bucephala albeola</i>
	<i>Bucephala albeola</i>		<i>Buteo lineatus</i>		<i>Geothlypis trichas</i>
	<i>Geothlypis trichas</i>		<i>Geothlypis trichas</i>		<i>Haliaeetus leucocephalus</i>
	<i>Larus delawarensis</i>		<i>Larus delawarensis</i>		<i>Leiothlypis celata</i>
	<i>Leiothlypis celata</i>		<i>Leiothlypis celata</i>		<i>Megaceryle alcyon</i>
	<i>Megaceryle alcyon</i>		<i>Melospiza melodia</i>		<i>Melospiza melodia</i>
	<i>Melospiza melodia</i>		<i>Setophaga coronata</i>		<i>Setophaga coronata</i>
	<i>Setophaga coronata</i>		<i>Setophaga palmarum</i>		<i>Turdus migratorius</i>
	<i>Spinus tristis</i>		<i>Turdus migratorius</i>		<i>Zonotrichia leucophrys</i>
271	<i>Turdus migratorius</i>	237	<i>Zonotrichia leucophrys</i>	236	<i>Branta canadensis</i>
	<i>Zonotrichia leucophrys</i>		<i>Aix sponsa</i>		
	<i>Branta canadensis</i>		<i>Branta canadensis</i>		
			<i>Leiothlypis ruficapilla</i>		
			<i>Molothrus ater</i>		
271	<i>Ardea alba</i>	237	<i>Catharus ustulatus</i>	236	<i>Catharus ustulatus</i>
	<i>Catharus ustulatus</i>		<i>Egretta thula</i>		<i>Hirundo rustica</i>
	<i>Hirundo rustica</i>		<i>Hirundo rustica</i>		<i>Myiarchus crinitus</i>
	<i>Icterus galbula</i>		<i>Myiarchus crinitus</i>		<i>Pandion haliaetus</i>
	<i>Myiarchus crinitus</i>		<i>Pandion haliaetus</i>		<i>Pheucticus ludovicianus</i>
	<i>Pandion haliaetus</i>		<i>Pheucticus ludovicianus</i>		<i>Setophaga petechia</i>
	<i>Pheucticus ludovicianus</i>		<i>Setophaga petechia</i>		<i>Sialia sialis</i>
	<i>Setophaga petechia</i>		<i>Sialia sialis</i>		<i>Spatula discors</i>
	<i>Sialia sialis</i>		<i>Spatula discors</i>		<i>Troglodytes aedon</i>
	<i>Spatula discors</i>		<i>Ardea alba</i>		<i>Icterus galbula</i>

Top 10 important stopovers		Potential alternative stopover sites			
Cell-ID	Species	Cell-ID	Species	Cell-ID	Species
624	<i>Buteo jamaicensis</i>	659	<i>Buteo lineatus</i>	694	<i>Buteo lineatus</i>
	<i>Buteo lineatus</i>		<i>Geothlypis trichas</i>		<i>Egretta thula</i>
	<i>Geothlypis trichas</i>		<i>Icterus galbula</i>		<i>Geothlypis trichas</i>
	<i>Leiothlypis ruficapilla</i>		<i>Myiarchus crinitus</i>		<i>Icterus galbula</i>
	<i>Myiarchus crinitus</i>		<i>Pandion haliaetus</i>		<i>Megaceryle alcyon</i>
	<i>Pandion haliaetus</i>		<i>Poliophtila caerulea</i>		<i>Myiarchus crinitus</i>
	<i>Pheucticus ludovicianus</i>		<i>Sayornis phoebe</i>		<i>Pandion haliaetus</i>
	<i>Podilymbus podiceps</i>		<i>Setophaga americana</i>		<i>Pheucticus ludovicianus</i>
	<i>Poliophtila caerulea</i>		<i>Setophaga coronata</i>		<i>Podilymbus podiceps</i>
	<i>Sayornis phoebe</i>		<i>Setophaga palmarum</i>		<i>Poliophtila caerulea</i>
	<i>Setophaga americana</i>		<i>Dumetella carolinensis</i>		<i>Sayornis phoebe</i>
	<i>Setophaga palmarum</i>		<i>Podilymbus podiceps</i>		<i>Setophaga americana</i>
	<i>Stelgidopteryx serripennis</i>		<i>Quiscalus quiscula</i>		<i>Setophaga coronata</i>
	<i>Dumetella carolinensis</i>		<i>Stelgidopteryx serripennis</i>		<i>Setophaga palmarum</i>
	<i>Icterus galbula</i>		<i>Buteo jamaicensis</i>		<i>Spizella passerina</i>
	<i>Spatula discors</i>		<i>Catharus ustulatus</i>		<i>Stelgidopteryx serripennis</i>
	<i>Catharus ustulatus</i>		<i>Hirundo rustica</i>		<i>Dumetella carolinensis</i>
	<i>Hirundo rustica</i>		<i>Leiothlypis ruficapilla</i>		<i>Pipilo erythrophthalmus</i>
	<i>Quiscalus quiscula</i>		<i>Megaceryle alcyon</i>		<i>Quiscalus quiscula</i>
			<i>Pheucticus ludovicianus</i>		<i>Toxostoma rufum</i>
			<i>Spizella passerina</i>		<i>Buteo jamaicensis</i>
					<i>Catharus ustulatus</i>
					<i>Hirundo rustica</i>
					<i>Passerina cyanea</i>
					<i>Sialia sialis</i>
236	<i>Catharus ustulatus</i>	235	<i>Hirundo rustica</i>	237	<i>Catharus ustulatus</i>
	<i>Hirundo rustica</i>		<i>Catharus ustulatus</i>		<i>Egretta thula</i>
	<i>Myiarchus crinitus</i>		<i>Setophaga petechia</i>		<i>Hirundo rustica</i>
	<i>Pandion haliaetus</i>				<i>Myiarchus crinitus</i>
	<i>Pheucticus ludovicianus</i>				<i>Pandion haliaetus</i>
	<i>Setophaga petechia</i>				<i>Pheucticus ludovicianus</i>
	<i>Sialia sialis</i>				<i>Setophaga petechia</i>
	<i>Spatula discors</i>				<i>Sialia sialis</i>
	<i>Troglodytes aedon</i>				<i>Spatula discors</i>
	<i>Icterus galbula</i>				<i>Ardea alba</i>
918	<i>Aix sponsa</i>	883	<i>Aix sponsa</i>	952	<i>Aix sponsa</i>
	<i>Anas platyrhynchos</i>		<i>Anas platyrhynchos</i>		<i>Anas platyrhynchos</i>
	<i>Bucephala albeola</i>		<i>Ardea herodias</i>		<i>Bucephala albeola</i>
	<i>Geothlypis trichas</i>		<i>Bucephala albeola</i>		<i>Geothlypis trichas</i>
	<i>Larus delawarensis</i>		<i>Geothlypis trichas</i>		<i>Larus delawarensis</i>
	<i>Leiothlypis celata</i>		<i>Leiothlypis celata</i>		<i>Leiothlypis celata</i>
	<i>Leiothlypis ruficapilla</i>		<i>Leiothlypis ruficapilla</i>		<i>Megaceryle alcyon</i>
	<i>Megaceryle alcyon</i>		<i>Pandion haliaetus</i>		<i>Melospiza melodia</i>
	<i>Melospiza melodia</i>		<i>Setophaga coronata</i>		<i>Setophaga coronata</i>
	<i>Pandion haliaetus</i>		<i>Setophaga palmarum</i>		<i>Spinus tristis</i>
	<i>Setophaga coronata</i>		<i>Sturnus vulgaris</i>		<i>Turdus migratorius</i>
	<i>Sturnus vulgaris</i>		<i>Zonotrichia leucophrys</i>		<i>Zonotrichia leucophrys</i>
	<i>Turdus migratorius</i>		<i>Branta canadensis</i>		<i>Branta canadensis</i>
	<i>Zonotrichia leucophrys</i>		<i>Melospiza melodia</i>		
	<i>Branta canadensis</i>		<i>Turdus migratorius</i>		
	<i>Colaptes auratus</i>		<i>Molothrus ater</i>		
	<i>Spinus tristis</i>				
	<i>Ardea herodias</i>				
	<i>Mareca strepera</i>				
	<i>Molothrus ater</i>				

Table S3. Cell-IDs with the included species for 2020-2022

Top 10 important stopovers		Potential alternative stopover sites			
Cell-ID	Species	Cell-ID	Species	Cell-ID	Species
237	<i>Catharus ustulatus</i> <i>Myiarchus crinitus</i> <i>Pandion haliaetus</i> <i>Pheucticus ludovicianus</i> <i>Setophaga petechia</i> <i>Spatula discors</i> <i>Hirundo rustica</i> <i>Icterus galbula</i> <i>Ardea alba</i>	236	<i>Catharus ustulatus</i> <i>Hirundo rustica</i> <i>Icterus galbula</i> <i>Pheucticus ludovicianus</i> <i>Setophaga petechia</i> <i>Myiarchus crinitus</i> <i>Spatula discors</i>	165	<i>Setophaga petechia</i>
589	<i>Archilochus colubris</i> <i>Buteo jamaicensis</i> <i>Dumetella carolinensis</i> <i>Geothlypis trichas</i> <i>Myiarchus crinitus</i> <i>Pandion haliaetus</i> <i>Pheucticus ludovicianus</i> <i>Poliophtila caerulea</i> <i>Quiscalus quiscula</i> <i>Sayornis phoebe</i> <i>Setophaga americana</i> <i>Setophaga palmarum</i> <i>Setophaga petechia</i> <i>Spatula discors</i> <i>Ardea herodias</i> <i>Catharus ustulatus</i> <i>Icterus galbula</i> <i>Leiothlypis ruficapilla</i> <i>Podilymbus podiceps</i> <i>Stelgidopteryx serripennis</i>	659	<i>Ardea herodias</i> <i>Buteo lineatus</i> <i>Dumetella carolinensis</i> <i>Geothlypis trichas</i> <i>Icterus galbula</i> <i>Myiarchus crinitus</i> <i>Pandion haliaetus</i> <i>Pheucticus ludovicianus</i> <i>Podilymbus podiceps</i> <i>Poliophtila caerulea</i> <i>Quiscalus quiscula</i> <i>Sayornis phoebe</i> <i>Setophaga americana</i> <i>Setophaga coronata</i> <i>Setophaga palmarum</i> <i>Setophaga petechia</i> <i>Spizella passerina</i> <i>Leiothlypis ruficapilla</i> <i>Sialia sialis</i> <i>Spatula discors</i> <i>Stelgidopteryx serripennis</i> <i>Toxostoma rufum</i> <i>Egretta thula</i>	624	<i>Buteo jamaicensis</i> <i>Buteo lineatus</i> <i>Dumetella carolinensis</i> <i>Geothlypis trichas</i> <i>Icterus galbula</i> <i>Leiothlypis ruficapilla</i> <i>Myiarchus crinitus</i> <i>Pandion haliaetus</i> <i>Pheucticus ludovicianus</i> <i>Poliophtila caerulea</i> <i>Quiscalus quiscula</i> <i>Sayornis phoebe</i> <i>Setophaga americana</i> <i>Setophaga palmarum</i> <i>Setophaga petechia</i> <i>Spatula discors</i> <i>Ardea herodias</i> <i>Podilymbus podiceps</i> <i>Stelgidopteryx serripennis</i>
554	<i>Archilochus colubris</i> <i>Buteo jamaicensis</i> <i>Dumetella carolinensis</i> <i>Egretta thula</i> <i>Myiarchus crinitus</i> <i>Pandion haliaetus</i> <i>Passerina cyanea</i> <i>Pheucticus ludovicianus</i> <i>Setophaga americana</i> <i>Setophaga palmarum</i> <i>Setophaga petechia</i> <i>Spatula discors</i> <i>Stelgidopteryx serripennis</i> <i>Ardea herodias</i> <i>Catharus ustulatus</i> <i>Fulica americana</i> <i>Icterus galbula</i> <i>Leiothlypis ruficapilla</i> <i>Poliophtila caerulea</i> <i>Quiscalus quiscula</i>	519	<i>Archilochus colubris</i> <i>Buteo jamaicensis</i> <i>Leiothlypis ruficapilla</i> <i>Myiarchus crinitus</i> <i>Passerina cyanea</i> <i>Podilymbus podiceps</i> <i>Setophaga americana</i> <i>Setophaga petechia</i> <i>Stelgidopteryx serripennis</i> <i>Ardea herodias</i> <i>Catharus ustulatus</i> <i>Pheucticus ludovicianus</i> <i>Setophaga palmarum</i> <i>Dumetella carolinensis</i> <i>Fulica americana</i> <i>Icterus galbula</i>	624	<i>Buteo jamaicensis</i> <i>Buteo lineatus</i> <i>Dumetella carolinensis</i> <i>Geothlypis trichas</i> <i>Icterus galbula</i> <i>Leiothlypis ruficapilla</i> <i>Myiarchus crinitus</i> <i>Pandion haliaetus</i> <i>Pheucticus ludovicianus</i> <i>Poliophtila caerulea</i> <i>Quiscalus quiscula</i> <i>Sayornis phoebe</i> <i>Setophaga americana</i> <i>Setophaga palmarum</i> <i>Setophaga petechia</i> <i>Spatula discors</i> <i>Ardea herodias</i> <i>Podilymbus podiceps</i> <i>Stelgidopteryx serripennis</i>

Top 10 important stopovers		Potential alternative stopover sites			
Cell-ID	Species	Cell-ID	Species	Cell-ID	Species
520	<i>Buteo jamaicensis</i>	519	<i>Archilochus colubris</i>	485	<i>Buteo jamaicensis</i>
	<i>Egretta thula</i>		<i>Buteo jamaicensis</i>		<i>Passerina cyanea</i>
	<i>Leiothlypis ruficapilla</i>		<i>Leiothlypis ruficapilla</i>		<i>Setophaga americana</i>
	<i>Passerina cyanea</i>		<i>Myiarchus crinitus</i>		<i>Setophaga petechia</i>
	<i>Setophaga americana</i>		<i>Passerina cyanea</i>		<i>Catharus ustulatus</i>
	<i>Setophaga petechia</i>		<i>Podilymbus podiceps</i>		<i>Fulica americana</i>
	<i>Catharus ustulatus</i>		<i>Setophaga americana</i>		<i>Pandion haliaetus</i>
	<i>Myiarchus crinitus</i>		<i>Setophaga petechia</i>		
	<i>Podilymbus podiceps</i>		<i>Stelgidopteryx serripennis</i>		
	<i>Fulica americana</i>		<i>Ardea herodias</i>		
	<i>Icterus galbula</i>		<i>Catharus ustulatus</i>		
	<i>Megasceryle alcyon</i>		<i>Pheucticus ludovicianus</i>		
	<i>Pandion haliaetus</i>		<i>Setophaga palmarum</i>		
	<i>Setophaga palmarum</i>		<i>Dumetella carolinensis</i>		
			<i>Fulica americana</i>		
			<i>Icterus galbula</i>		
519	<i>Archilochus colubris</i>	520	<i>Buteo jamaicensis</i>	485	<i>Buteo jamaicensis</i>
	<i>Buteo jamaicensis</i>		<i>Egretta thula</i>		<i>Passerina cyanea</i>
	<i>Leiothlypis ruficapilla</i>		<i>Leiothlypis ruficapilla</i>		<i>Setophaga americana</i>
	<i>Myiarchus crinitus</i>		<i>Passerina cyanea</i>		<i>Setophaga petechia</i>
	<i>Passerina cyanea</i>		<i>Setophaga americana</i>		<i>Catharus ustulatus</i>
	<i>Podilymbus podiceps</i>		<i>Setophaga petechia</i>		<i>Fulica americana</i>
	<i>Setophaga americana</i>		<i>Catharus ustulatus</i>		<i>Pandion haliaetus</i>
	<i>Setophaga petechia</i>		<i>Myiarchus crinitus</i>		
	<i>Stelgidopteryx serripennis</i>		<i>Podilymbus podiceps</i>		
	<i>Ardea herodias</i>		<i>Fulica americana</i>		
	<i>Catharus ustulatus</i>		<i>Icterus galbula</i>		
	<i>Pheucticus ludovicianus</i>		<i>Megasceryle alcyon</i>		
	<i>Setophaga palmarum</i>		<i>Pandion haliaetus</i>		
	<i>Dumetella carolinensis</i>		<i>Setophaga palmarum</i>		
	<i>Fulica americana</i>				
	<i>Icterus galbula</i>				
952	<i>Aix sponsa</i>	917	<i>Anas platyrhynchos</i>	987	<i>Aix sponsa</i>
	<i>Bucephala albeola</i>		<i>Branta canadensis</i>		<i>Branta canadensis</i>
	<i>Buteo lineatus</i>		<i>Bucephala albeola</i>		<i>Bucephala albeola</i>
	<i>Geothlypis trichas</i>		<i>Buteo lineatus</i>		<i>Colaptes auratus</i>
	<i>Leiothlypis celata</i>		<i>Leiothlypis celata</i>		<i>Geothlypis trichas</i>
	<i>Megasceryle alcyon</i>		<i>Melospiza melodia</i>		<i>Icterus galbula</i>
	<i>Melospiza melodia</i>		<i>Spinus tristis</i>		<i>Leiothlypis celata</i>
	<i>Spinus tristis</i>		<i>Turdus migratorius</i>		<i>Megasceryle alcyon</i>
	<i>Turdus migratorius</i>		<i>Zonotrichia leucophrys</i>		<i>Melospiza melodia</i>
	<i>Zonotrichia leucophrys</i>		<i>Aix sponsa</i>		<i>Spinus tristis</i>
	<i>Anas platyrhynchos</i>		<i>Megasceryle alcyon</i>		<i>Turdus migratorius</i>
					<i>Zonotrichia leucophrys</i>
					<i>Anas platyrhynchos</i>
					<i>Haliaeetus leucocephalus</i>
					<i>Larus delawarensis</i>
271	<i>Catharus ustulatus</i>	237	<i>Catharus ustulatus</i>	236	<i>Catharus ustulatus</i>
	<i>Hirundo rustica</i>		<i>Myiarchus crinitus</i>		<i>Hirundo rustica</i>
	<i>Icterus galbula</i>		<i>Pandion haliaetus</i>		<i>Icterus galbula</i>
	<i>Myiarchus crinitus</i>		<i>Pheucticus ludovicianus</i>		<i>Pheucticus ludovicianus</i>
	<i>Pandion haliaetus</i>		<i>Setophaga petechia</i>		<i>Setophaga petechia</i>
	<i>Pheucticus ludovicianus</i>		<i>Spatula discors</i>		<i>Myiarchus crinitus</i>
	<i>Setophaga petechia</i>		<i>Hirundo rustica</i>		<i>Spatula discors</i>
	<i>Spatula discors</i>		<i>Icterus galbula</i>		
	<i>Stelgidopteryx serripennis</i>		<i>Ardea alba</i>		
	<i>Ardea alba</i>				
	<i>Spizella passerina</i>				

Top 10 important stopovers		Potential alternative stopover sites			
Cell-ID	Species	Cell-ID	Species	Cell-ID	Species
624	<i>Buteo jamaicensis</i>	659	<i>Ardea herodias</i>	694	<i>Ardea herodias</i>
	<i>Buteo lineatus</i>		<i>Buteo lineatus</i>		<i>Buteo lineatus</i>
	<i>Dumetella carolinensis</i>		<i>Dumetella carolinensis</i>		<i>Dumetella carolinensis</i>
	<i>Geothlypis trichas</i>		<i>Geothlypis trichas</i>		<i>Egretta thula</i>
	<i>Icterus galbula</i>		<i>Icterus galbula</i>		<i>Geothlypis trichas</i>
	<i>Leiothlypis ruficapilla</i>		<i>Myiarchus crinitus</i>		<i>Icterus galbula</i>
	<i>Myiarchus crinitus</i>		<i>Pandion haliaetus</i>		<i>Megaceryle alcyon</i>
	<i>Pandion haliaetus</i>		<i>Pheucticus ludovicianus</i>		<i>Myiarchus crinitus</i>
	<i>Pheucticus ludovicianus</i>		<i>Podilymbus podiceps</i>		<i>Pandion haliaetus</i>
	<i>Poliophtila caerulea</i>		<i>Poliophtila caerulea</i>		<i>Podilymbus podiceps</i>
	<i>Quiscalus quiscula</i>		<i>Quiscalus quiscula</i>		<i>Poliophtila caerulea</i>
	<i>Sayornis phoebe</i>		<i>Sayornis phoebe</i>		<i>Quiscalus quiscula</i>
	<i>Setophaga americana</i>		<i>Setophaga americana</i>		<i>Sayornis phoebe</i>
	<i>Setophaga palmarum</i>		<i>Setophaga coronata</i>		<i>Setophaga americana</i>
	<i>Setophaga petechia</i>		<i>Setophaga palmarum</i>		<i>Setophaga petechia</i>
	<i>Spatula discors</i>		<i>Setophaga petechia</i>		<i>Spizella passerina</i>
	<i>Ardea herodias</i>		<i>Spizella passerina</i>		<i>Leiothlypis ruficapilla</i>
	<i>Podilymbus podiceps</i>		<i>Leiothlypis ruficapilla</i>		<i>Setophaga coronata</i>
	<i>Stelgidopteryx serripennis</i>		<i>Sialia sialis</i>		<i>Sialia sialis</i>
			<i>Spatula discors</i>		<i>Toxostoma rufum</i>
			<i>Stelgidopteryx serripennis</i>		<i>Setophaga palmarum</i>
			<i>Toxostoma rufum</i>		<i>Turdus migratorius</i>
			<i>Egretta thula</i>		
236	<i>Catharus ustulatus</i>	235	<i>Catharus ustulatus</i>	237	<i>Catharus ustulatus</i>
	<i>Hirundo rustica</i>		<i>Hirundo rustica</i>		<i>Myiarchus crinitus</i>
	<i>Icterus galbula</i>		<i>Icterus galbula</i>		<i>Pandion haliaetus</i>
	<i>Pheucticus ludovicianus</i>	237			<i>Pheucticus ludovicianus</i>
	<i>Setophaga petechia</i>				<i>Setophaga petechia</i>
	<i>Myiarchus crinitus</i>				<i>Spatula discors</i>
	<i>Spatula discors</i>				<i>Hirundo rustica</i>
918		883		952	<i>Icterus galbula</i>
					<i>Ardea alba</i>
	<i>Aix sponsa</i>		<i>Aix sponsa</i>		
	<i>Ardea herodias</i>		<i>Anas platyrhynchos</i>		<i>Aix sponsa</i>
	<i>Branta canadensis</i>		<i>Ardea herodias</i>		<i>Bucephala albeola</i>
	<i>Bucephala albeola</i>		<i>Branta canadensis</i>		<i>Buteo lineatus</i>
	<i>Colaptes auratus</i>		<i>Bucephala albeola</i>		<i>Geothlypis trichas</i>
	<i>Geothlypis trichas</i>		<i>Colaptes auratus</i>		<i>Leiothlypis celata</i>
	<i>Megaceryle alcyon</i>		<i>Geothlypis trichas</i>		<i>Megaceryle alcyon</i>
	<i>Melospiza melodia</i>		<i>Megaceryle alcyon</i>		<i>Melospiza melodia</i>
	<i>Pandion haliaetus</i>		<i>Molothrus ater</i>		<i>Spinus tristis</i>
	<i>Spinus tristis</i>		<i>Spinus tristis</i>		<i>Turdus migratorius</i>
	<i>Sturnus vulgaris</i>		<i>Sturnus vulgaris</i>		<i>Zonotrichia leucophrys</i>
	<i>Turdus migratorius</i>		<i>Turdus migratorius</i>		<i>Anas platyrhynchos</i>
	<i>Zonotrichia leucophrys</i>		<i>Zonotrichia leucophrys</i>		
	<i>Anas platyrhynchos</i>		<i>Leiothlypis celata</i>		
	<i>Leiothlypis celata</i>		<i>Leiothlypis ruficapilla</i>		
	<i>Leiothlypis ruficapilla</i>		<i>Melospiza melodia</i>		
	<i>Molothrus ater</i>		<i>Setophaga coronata</i>		
	<i>Setophaga coronata</i>				